


RESEARCH ARTICLE

Connexin 43 hemichannels and pannexin-1 channels contribute to the α -synuclein-induced dysfunction and death of astrocytes

Esteban F. Díaz¹ | Valeria C. Labra¹ | Tanhia F. Alvear¹ | Luis A. Mellado¹ |
Carla A. Inostroza¹ | Juan E. Oyarzún¹ | Nicole Salgado² | Rodrigo A. Quintanilla^{3,4} |
Juan A. Orellana^{1,3} 

¹Departamento de Neurología, Escuela de Medicina and Centro Interdisciplinario de Neurociencias, Facultad de Medicina, Pontificia Universidad Católica de Chile, Santiago, Chile

²Unidad de Microscopía Avanzada UC, Facultad de Ciencias Biológicas, Pontificia Universidad Católica de Chile, Santiago, Chile

³Escuela de Medicina, Centro de Investigación y Estudio del Consumo de Alcohol en Adolescentes (CIAA), Santiago, Chile

⁴Laboratory of Neurodegenerative Diseases, Universidad Autónoma de Chile, Santiago, Chile

Correspondence

Juan A. Orellana, PhD, Departamento de Neurología, Escuela de Medicina, Pontificia Universidad Católica de Chile, Marcoleta 391, Santiago, Chile.
Email: jaorella@uc.cl

Funding information

Comisión Nacional de Investigación Científica y Tecnológica (CONICYT) and Programa de Investigación Asociativa (PIA), Grant/Award Number: ACT1411; Fondo Nacional de Desarrollo Científico y Tecnológico (FONDECYT), Grant/Award Numbers: 1160710, 1170441

Abstract

Diverse studies have suggested that cytoplasmic inclusions of misfolded α -synuclein in neuronal and glial cells are main pathological features of different α -synucleinopathies, including Parkinson's disease and dementia with Lewy bodies. Up to now, most studies have focused on the effects of α -synuclein on neurons, whereas the possible alterations of astrocyte functions and neuron–glia crosstalk have received minor attention. Recent evidence indicates that cellular signaling mediated by hemichannels and pannexons is critical for astroglial function and dysfunction. These channels constitute a diffusional route of communication between the cytosol and the extracellular space and during pathological scenarios they may lead to homeostatic disturbances linked to the pathogenesis and progression of different diseases. Here, we found that α -synuclein enhances the opening of connexin 43 (Cx43) hemichannels and pannexin-1 (Panx1) channels in mouse cortical astrocytes. This response was linked to the activation of cytokines, the p38 MAP kinase, the inducible nitric oxide synthase, cyclooxygenase 2, intracellular free Ca^{2+} concentration ($[\text{Ca}^{2+}]_i$), and purinergic and glutamatergic signaling. Relevantly, the α -synuclein-induced opening of hemichannels and pannexons resulted in alterations in $[\text{Ca}^{2+}]_i$ dynamics, nitric oxide (NO) production, gliotransmitter release, mitochondrial morphology, and astrocyte survival. We propose that α -synuclein-mediated opening of astroglial Cx43 hemichannels and Panx1 channels might constitute a novel mechanism involved in the pathogenesis and progression of α -synucleinopathies.

KEYWORDS

connexin, glia, neuroinflammation, pannexin, α -synucleinopathies

1 | INTRODUCTION

α -Synuclein is a 14 kDa acidic soluble unfolded protein that participates in synaptic vesicle turnover and neurotransmitter release (Bendor, Logan, & Edwards, 2013). A profound revolution began when two pioneering findings clearly linked α -synuclein to Parkinson's disease

(PD): (a) the discovery that a missense mutation of the gene encoding α -synuclein is pathogenic for a rare familial form of PD (Polymeropoulos et al., 1997) and (b) the revelation that α -synuclein is the principal component of Lewy bodies (LBs) and Lewy neurites in sporadic PD (Spillantini et al., 1997). Nowadays, the cytoplasmic inclusions of misfolded α -synuclein are considered the main pathological

features of different α -synucleinopathies, including PD, dementia with LBs, multiple system atrophy, Alzheimer's disease, and neurodegeneration with brain iron accumulation Type 1 (Vekrellis, Xilouri, Emmanouilidou, Rideout, & Stefanis, 2011).

Despite the continuous ongoing research in the field, the cellular and molecular mechanisms underlying the pathological action of α -synuclein remain to be fully elucidated. Up to now, most studies have focused on the effects of α -synuclein in neurons, whereas the possible alterations of glial cells and neuron–glia crosstalk have received minor attention. Astrocytes are the most numerous glial cell type in the CNS and embedded in the synaptic cleft, they sense neuronal activity and respond to it by releasing bioactive molecules termed “gliotransmitters” (e.g., glutamate, ATP, and D-serine; Perea, Navarrete, & Araque, 2009). In addition to their synaptic role, astrocytes are key players in supplying energy to neurons (lactate), maintaining the homeostatic balance of extracellular pH, neurotransmitters, and ions, as well as controlling the redox response and Ca^{2+} signaling (Volterra, Liaudet, & Savtchouk, 2014). Nevertheless, many brain disorders cause astrocyte changes collectively referred to as “reactive astrogliosis” (Pekny & Pekna, 2014). This phenomenon constitutes a graded and multistage astroglial cell reaction that counteracts acute damage, restoring homeostasis, and limiting brain parenchyma injury (Pekny & Pekna, 2014). Although this response is usually neuroprotective, when it turns persistent, impairs gliotransmission, Ca^{2+} signaling, and mitochondrial function, as well as elevates NO production, and recruitment of the innate immune response (Pekny & Pekna, 2014).

Overexpression or in vitro or in vivo administration of α -synuclein induces reactive astrogliosis accompanied of enhanced GFAP expression, mitochondrial dysfunction, and cell death (Fellner et al., 2013; Klegeris et al., 2006; Koob, Paulino, & Masliah, 2010). Nonetheless, the mechanisms that account for these changes and whether other astrocytic functions (e.g., gliotransmitter release and Ca^{2+} dynamics) are altered remain unknown. Recent findings suggest that cellular signaling mediated by hemichannels and pannexons might contribute to the dysfunction of astrocytes (Orellana, Retamal, Moraga-Amaro, & Stehberg, 2016). Hemichannels are plasma membrane channels constituted of six connexin monomers that oligomerize around a central pore that allow the passage of ions and small molecules, serving as a diffusional route of communication between the cytosol and the extracellular space (Montero & Orellana, 2015). At the other end, pannexins channels or pannexons result from the oligomerization of pannexins, a three-member family of proteins that have equivalent secondary and tertiary structures than connexins with the ability to form plasma membrane channels (Iglesias, Dahl, Qiu, Spray, & Scemes, 2009). Although the opening of hemichannels has been proposed as a mechanism of gliotransmission linked to synaptic transmission, plasticity, and memory (Chever, Lee, & Rouach, 2014; Meunier et al., 2017; Stehberg et al., 2012), other studies have raised doubts about the hypothetical role of hemichannels under physiological conditions (Nielsen, Hansen, Ransom, Nielsen, & Macaulay, 2017). Despite the data status about this matter is still inconclusive in the connexin field, what seems most clear is the participation of hemichannels and pannexons in the homeostatic disturbances

linked to the pathogenesis and progression of different diseases (Leybaert et al., 2017; Orellana et al., 2016; Salameh, Blanke, & Dhein, 2013).

Here, we show that α -synuclein enhances the opening of connexin 43 (Cx43) hemichannels and pannexin-1 (Panx1) channels in mouse cortical astrocytes. This response was linked to the activation of cytokines, the p38 MAP kinase, the inducible nitric oxide synthase (iNOS), cyclooxygenase 2 (COX₂), intracellular free Ca^{2+} concentration ($[\text{Ca}^{2+}]_i$), and purinergic and glutamatergic signaling. Astrocytes treated for 24 hr with α -synuclein exhibited an increased ethidium (Etd) uptake and release of glutamate and ATP when compared to control conditions. Relevantly, the α -synuclein-induced opening of hemichannels and pannexons resulted in alterations in $[\text{Ca}^{2+}]_i$ dynamics, nitric oxide (NO) production, gliotransmitter release, mitochondrial morphology, and astrocyte survival.

2 | MATERIALS AND METHODS

2.1 | Reagents and antibodies

Gap19 (KQIEIKKFK, intracellular loop domain of Cx43), Tat-L2 (YGRKKRRQRRRDGANVDMHLKQIEIKKFKYGIEEHGK, second intracellular loop domain of Cx43), and ¹⁰panx1 (WRQAAFVDSY, first extracellular loop domain of Panx1) peptides were obtained from Genscript (Piscataway, NJ). HEPES, water (W3500), DMEM, DNase I, poly-L-lysine, L-N6, SB203580, anti-Cx43 polyclonal antibody, anti-GFAP monoclonal antibody, Lucifer yellow (LY), Etd bromide, wild-type α -synuclein, and probenecid (Prob) were purchased from Sigma-Aldrich (St. Louis, MO). Fetal bovine serum (FBS) was obtained from Hyclone (Logan, UT). Penicillin, streptomycin, polyclonal anti-Panx1 antibody (PI488000), FURA-2AM, BAPTA-AM, Mito Green 488, DAF-FM, hoechst 33342, Etd homodimer-1 (EthD-1), wheat germ agglutinin (WGA) Alexa Fluor™ 555 Conjugate, goat anti-mouse Alexa Fluor 488/555, and goat anti-rabbit Alexa Fluor 488/555 were obtained from Thermo Fisher Scientific (Waltham, MA). Anti-Panx1 monoclonal antibody was purchased from Abcam (Cambridge, UK). Normal goat serum (NGS) was purchased from Zymed (San Francisco, CA). Anti-Cx43 monoclonal antibody (610061) was obtained from BD Biosciences (Franklin Lakes, NJ). Anti-phospho-Cx43 (Ser368) polyclonal antibody (AB_2110169) was obtained from Cell Signaling Technologies (Danvers, MA). IL-1 β and TNF- α were obtained from Roche Diagnostics (Indianapolis, MI). A soluble form of the TNF- α receptor (sTNF- α R1) and a recombinant receptor antagonist for IL-1 β (IL-1ra) were from R&D Systems (Minneapolis, MN). Horseradish peroxidase (HRP)-conjugated anti-rabbit IgG was purchased from Pierce (Rockford, IL).

2.2 | Animals

Animal experimentation was conducted in accordance with the guideline for care and use of experimental animals of the US National Institutes of Health (NIH, Bethesda, MD), the ad hoc committee of the Chilean government (CONICYT), the Bioethics Committee of the Pontificia Universidad Católica de Chile (PUC), and the European Community

Council Directives of November 24th, 1986. C57BL/6 (PUC) mice of 8–9 weeks of age were housed in cages in a temperature-controlled (24 °C) and humidity-controlled vivarium under a 12 hr light/dark cycle (lights on 8:00 a.m.), with ad libitum access to food and water.

2.3 | Cell cultures

Astroglial cell primary cultures were prepared from cortex of postnatal Day 2 (P2) mice as previously described (Avendano, Montero, Chavez, Von Bernhardi, & Orellana, 2015). Briefly, brains were removed, and cortices were dissected. Meninges were carefully peeled off and tissue was mechanically dissociated in Ca²⁺ and Mg²⁺ free Hank's balanced salt solution (CM-HBSS) with 0.25% trypsin and 1% DNase. Cells were seeded onto 60-mm plastic dishes (Falcon) or onto glass coverslips (Gassalem, Limeil-Brevannes, France) placed inside 16-mm 24-well plastic plates (Falcon) at the density of 2×10^6 cells/dish or 1×10^5 cells/well, respectively, in DMEM, supplemented with penicillin (5 U/mL), streptomycin (5 µg/mL), and 10% FBS. Cells were grown at 37 °C in a 5% CO₂/95% air atmosphere at nearly 100% relative humidity. After 8–10 days in vitro (DIV), 1 µM cytosine-arabioside was added for 3 days to eliminate proliferating microglia. Medium was changed twice a week and cultures were used after 3 weeks. At that stage, these cultures contained >97% GFAP+ cells. No neurons were detected as judged by MAP2 and NeuN staining.

2.4 | Treatments

Astrocytes were treated for 0, 1, 24, or 48 hr with 0.1, 1, 10, or 100 nM of α -synuclein solubilized in PBS and incubated or "aged" at 37 °C with agitation for 0, 7, or 21 days, as previously described to generate monomers, oligomers, or fibrils, respectively (Diogenes et al., 2012; Fellner et al., 2013; Zhang et al., 2005). The protein preparations were rapidly stored at –80 °C. To obtain conditioned media (CM) from astrocytes, cells were seeded (2×10^6 cells in 35 mm dishes) in DMEM containing 10% FBS and treated with 10 nM α -synuclein for 24 hr. Supernatants were collected, filtered (0.22 µm), and stored at –20 °C before used for experiments. The following pharmacological agents were preincubated 1 hr prior and coincubated with 10 nM α -synuclein before experiments: Mimetic peptides against Cx43 hemichannels (Tat-L2 and gap19, 100 µM) and pannexin1 (Panx1) channels (¹⁰panx1, 100 µM), Prob (pannexin channel blocker, 500 µM), sTNF- α R1 (soluble form of the receptor that binds TNF- α), IL-1ra (IL-1 β receptor endogenous blocker), SB203580 (p38 MAP kinase inhibitor, 1 µM), L-N6 (iNOS inhibitor, 1 µM), sc-560 (inhibitor of COX₁, 20 nM), ns-398 (COX₂ inhibitor, 5 µM), sc-19,220 (EP₁ prostanoid receptor antagonist, 20 µM), BAPTA-AM (intracellular Ca²⁺ chelator, 10 µM), oATP (general P2X receptor blocker, 200 µM), MRS2179 (P2Y₁ receptor blocker, 1 µM), A740003 (P2X₇ receptor blocker, 200 nM), LY341495 (selective antagonist of group II metabotropic glutamate receptors [mGluR_{2/3}], 100 nM), D-AP5 (selective NMDA receptor antagonist, 1 µM), CPP (selective NMDA receptor antagonist, 1 µM), MTEP (selective mGluR₅ antagonist, 50 nM), SIB-1757 (selective mGluR₅ antagonist, 5 µM), and TGN-020 (selective aquaporin4 [AQP4] antagonist, 15 µM).

2.5 | siRNA transfection

siRNA duplexes against mouse Cx43 or Panx1 were predesigned and obtained from Origene (Rockville, MD). siRNA (10 nM) was transfected with Oligofectamine (Invitrogen) according to the Origene application guide for Trilencer-27 siRNA. Negligible cell death was detected after transfection (data not shown). Sequences for siRNAs against mouse Cx43 and Panx1 were: siRNA-Cx43: rGrCrArGrUrGrCrArCrArUrGrUrArArCrUrArArUrUrUrATT and siRNA-Panx1: rArGrArCrArUrArArGrUrGrArGrCrUrCrArArArUrCrGTA, respectively. Transfection experiments were performed 48 hr before the treatment with 10 nM α -synuclein for 24 hr.

2.6 | Dye uptake and time-lapse fluorescence imaging

For time-lapse fluorescence imaging, astrocytes plated on glass coverslips were washed twice in Hank's balanced salt solution. Then, cells were incubated at room temperature with Locke's solution with 5 µM Etd and mounted on the stage of an Olympus BX 51W11 upright microscope with a 40 \times water immersion objective for time-lapse imaging. Images were captured by a Retiga 1300I fast-cooled monochromatic digital camera (12-bit; Qimaging, Burnaby, BC, Canada) controlled by imaging software Metafluor software (Universal Imaging, Downingtown, PA) every 30 s (exposure time = 0.5 s; excitation and emission wavelengths were 528 and 598 nm, respectively). The fluorescence intensity recorded from 25 regions of interest (representing 25 cells per cultured coverslip) was calculated with the following formula: Corrected total cell Etd fluorescence = Integrated Density – ([Area of selected cell] \times [Mean fluorescence of background readings]). The mean slope of the relationship over a given time interval ($\Delta F/\Delta T$) represents the Etd uptake rate. To assess for changes in slope, regression lines were fitted to points before and after the various experimental conditions using Excel program, and mean values of slopes were compared using GraphPad Prism software and expressed as AU/min. At least three replicates (four sister cultured coverslips) were measured in each independent experiment. In some experiments, cultured astrocytes were preincubated with synthetic mimetic peptides Tat-L2 (100 µM), gap19 (100 µM), and ¹⁰panx1 (100 µM) for 15 min before and during the time-lapse experiments of Etd uptake.

2.7 | Western blot analysis

Astrocytes were rinsed twice with PBS (pH 7.4) and harvested by scraping with a rubber policeman in ice-cold PBS containing 5 mM EDTA, Halt (78440), and M-PER protein extraction cocktail (78501) according to the manufacturer instructions (Pierce, Rockford, IL). The cell suspension was sonicated on ice. Proteins were measured using the Bio-Rad protein assay. Aliquots of cell lysates (100 µg of protein) were resuspended in Laemli's sample buffer, separated in an 8% sodium dodecyl sulfate-polyacrylamide gel electrophoresis (SDS-PAGE) and electrotransferred to nitrocellulose sheets. Nonspecific protein binding was blocked by incubation of nitrocellulose sheets in

PBS-BLOTTO (5% nonfat milk in PBS) for 30 min. Blots were then incubated with primary antibody at 4 °C overnight, followed by four 15 min washes with PBS. Then, blots were incubated with HRP-conjugated goat anti-rabbit antibody at room temperature for 1 hr and then rinsed four times with PBS for 15 min. Immunoreactivity was detected by enhanced chemiluminescence (ECL) detection using the SuperSignal kit (Pierce, Rockford, IL) according to the manufacturer's instructions.

2.8 | Scrape loading/dye diffusion technique

Gap junction permeability was evaluated at room temperature using the scrape-loading/dye transfer (SL/DT) technique. Briefly, astroglial cultures were washed for 10 min in HEPES-buffered salt solution containing the following (in mM): 140 NaCl, 5.5 KCl, 1.8 CaCl₂, 1 MgCl₂, 5 glucose, 10 HEPES, pH 7.4 followed by washing in a Ca²⁺-free HEPES solution for 1 min. Then, a razor blade cut was made in the monolayer in a HEPES-buffered salt solution with normal Ca²⁺ concentration containing the fluorescent dye LY. After 1 min, LY (100 μM) was washed out several times with HEPES-buffered salt solution. At 8 min after scraping, fluorescent images were captured using an Olympus BX 51W1I upright microscope with a 40× water immersion objective. Changes were monitored using an imaging system equipped with a Retga 1300I fast-cooled monochromatic digital camera (12-bit; Qimaging, Burnaby, BC, Canada), monochromator for fluorophore excitation, and Metafluor software (Universal Imaging, Downingtown, PA) for image acquisition and analysis. For each trial, data were quantified by measuring fluorescence areas in three representative fields. Quantification of changes in gap junctional communication induced by different treatments was performed by measuring the fluorescence area, expressed as arbitrary units (AU).

2.9 | Immunofluorescence and confocal microscopy

Astrocytes grown on coverslips were fixed at room temperature with 2% paraformaldehyde (PFA) for 30 min and then washed three times with PBS. They were incubated three times for 5 min in 0.1 M PBS-glycine, and then in 0.1% PBS-Triton X-100 containing 10% NGS for 30 min. Cells were incubated with anti-GFAP monoclonal antibody (Sigma, 1:400), anti-Cx43 polyclonal antibody (SIGMA, 1:400) and anti-Panx1 monoclonal antibody (ABCAM 1:400) diluted in 0.1% PBS-Triton X-100 with 2% NGS at 4 °C overnight. After five rinses in 0.1% PBS-Triton X-100, cells were incubated with goat anti-mouse IgG Alexa Fluor 355 (1:1000) or goat anti-rabbit IgG Alexa Fluor 488 (1:1000) at room temperature for 50 min. After several rinses, coverslips were mounted in DAKO fluorescent mounting medium and examined with an Olympus BX 51W1I upright microscope with a 40× water immersion or a confocal system Nikon Eclipse C2 up microscope with 60×. In a set of experiments, the plasma membrane of astrocytes was stained with Wheat-germ agglutinin (WGA) labeled with Alexa Fluor 555 (5 μg/mL) for 15 min at 37 °C before fixation with PFA. Nuclei were stained with DAPI or Hoechst 33342. To assess the fluorescent intensity of Cx43 or Panx1 in the plasma membrane area labeled with WGA, stacks of

consecutive confocal images were taken with a confocal system Nikon Eclipse C2 up microscope and a 60X oil immersion objective (1.4 NA) at 200 nm intervals. Images were acquired sequentially with three lasers (in nm: 408, 488, and 543), and Z projections were reconstructed using Nikon confocal software (NIS-elements). Image analysis of Z projections was then performed with ImageJ software. Cx43 or Panx1 signal intensity in both plasma membrane and cytoplasm was calculated with the following formula: Corrected cell stain fluorescence = Integrated Density - ([Area of selected cell] x [Mean fluorescence of background readings]). Images obtained by Z projections of a selection of three out of the total number of the serial optical sections are shown in each figure: The selected sections are all central and crossing the nucleus visualized by DAPI staining. The mean ± standard error of signal staining was calculated analyzing a minimum of 50 cells for each treatment randomly taken from three independent experiments.

2.10 | [Ca²⁺]_i and NO imaging

Astrocytes plated on glass coverslips were loaded with 5 μM Fura-2-AM or 5 μM DAF-FM in DMEM without serum at 37 °C for 45 min and then washed three times in Locke's solution (154 mM NaCl, 5.4 mM KCl, 2.3 mM CaCl₂, 5 mM HEPES, pH 7.4) followed by deesterification at 37 °C for 15 min. The experimental protocol for [Ca²⁺]_i and nitric oxide (NO) imaging involved data acquisition every 5 s (emission at 510 and 515 nm, respectively) at 340/380 nm and 495 nm excitation wavelengths, respectively, using an Olympus BX 51W1I upright microscope with a 40× water immersion objective at room temperature. Changes were monitored using an imaging system equipped with a Retga 1300I fast-cooled monochromatic digital camera (12-bit; Qimaging, Burnaby, BC, Canada), monochromator for fluorophore excitation, and METAFLUOR software (Universal Imaging, Downingtown, PA) for image acquisition and analysis. Analysis involved determination of pixels assigned to each cell. The average pixel value allocated to each cell was obtained with excitation at each wavelength and corrected for background. Due to the low excitation intensity, no bleaching was observed even when cells were illuminated for a few minutes. The FURA-2AM ratio was obtained after dividing the 340-nm by the 380-nm fluorescence image on a pixel-by-pixel base ($R = F_{340 \text{ nm}}/F_{380 \text{ nm}}$).

2.11 | Quantification of mitochondrial length

The length of individual mitochondria was measured with the fluorescent probe MitoGreen. Briefly, cells were loaded with MitoGreen (1 μM) at 37 °C for 30 min in Krebs-Ringer-HEPES (KRH; 136 mM NaCl, 20 mM HEPES, 4.7 mM KCl, 1.5 mM MgSO₄, 1.25 mM CaCl₂, 5 mM glucose; pH = 7.4). The experimental protocol for MitoGreen imaging involved data acquisition at 490 nm excitation and 516 nm emission wavelengths, using an epifluorescence microscopy (Leica LX6000, Germany) with a 63× oil objective at room temperature. For mitochondrial length measurements, ImageJ software was used and calibrated using the scale determined by the Leica Application Suite software (Leica, Germany) when images were captured. Quantitative

analysis involved the measurement of at least 20 mitochondria per cell from a total population of 20 cells for each experiment.

2.12 | IL-1 β and TNF- α determination assay

IL-1 β and TNF- α were determined in the astrocyte CM. Samples were centrifuged at 14,000g for 40 min. Supernatants were collected and protein content assayed by the BCA method. IL-1 β and TNF- α levels were determined by sandwich ELISA, according to the manufacturer's protocol (eBioscience, San Diego, CA). For the assay, 100 μ L of samples were added per ELISA plate well and incubated at 4 °C overnight. A calibration curve with recombinant cytokine was included. Detection antibody was incubated at room temperature for 1 hr and the reaction developed with avidin-HRP and substrate solution. Absorbance was measured at 450 nm with reference to 570 nm with the microplate reader Synergy HT (BioTek Instruments, Winooski, VT).

2.13 | Measurement of extracellular ATP and glutamate concentration

Extracellular ATP in CM of astrocytes was measured using a luciferin/luciferase bioluminescence assay kit (Sigma-Aldrich), while extracellular levels of glutamate were determined using an enzyme-linked fluorimetric assay (Sigma-Aldrich). For measurements of intracellular ATP and glutamate levels, cells were lysed with Tris-buffered solution containing 1% TritonX-100 and supernatants of whole-cell lysates were used. The amounts of ATP in the samples were calculated from standard curves and normalized for the protein concentration, using the Bio-Rad protein assay.

2.14 | Astrocyte death quantification

Astrocyte membrane breakdown was evaluated by incorporation of the cell-impermeant viability indicator Ethidium homodimer-1 (EthD-1). Briefly, cells were incubated with Hank's balanced salt solution with EthD-1 (5 μ M) and Hoechst 33342 (1 μ M) at 37 °C for 15 min and then washed three times in PBS. Hoechst 33342 and EthD-1 imaging involved data acquisition (emission at 350 and 528 nm, respectively) at 461 and 628 nm excitation wavelengths, respectively, using an Olympus BX 51W11 upright microscope with a 40 \times water immersion objective. The quantification of cell death was expressed as the percentage of cells that incorporated EthD-1 (red cells) in relation of total cell population (blue cells) in each image captured. A total of 15 images (20–30 cells per image) for each experiment were analyzed using the ImageJ software.

2.15 | Dye uptake in acute brainstem slices

Mice were anesthetized under isoflurane, decapitated and brainstem was extracted, and cut into coronal slices (300 μ m) using a vibratome (Leica, VT1000GS; Leica, Wetzlar, Germany) filled with ice-cold slicing solution containing (in mM): Sucrose (222); KCl (2.6); NaHCO₃ (27); NaHPO₄ (1.5); glucose (10); MgSO₄ (7); CaCl₂ (0.5) and ascorbate

(0.1), and bubbled with 95% O₂/5% CO₂, pH 7.4. Then, the slices were transferred at room temperature (20–22 °C) to a holding chamber in ice-cold artificial cerebral spinal fluid (ACSF) containing (in mM): NaCl (125), KCl (2.5), glucose (25), NaHCO₃ (25), NaH₂PO₄ (1.25), CaCl₂ (2), and MgCl₂ (1), bubbled with 95% O₂/5% CO₂, pH 7.4, for a stabilization period of 60 min before dye uptake experiments (see below). For dye uptake and ex vivo "snapshot" experiments, acute brainstem slices were incubated with 5 μ M Etd for 10 min in a chamber filled with ACSF and bubbled with 95% O₂/5% CO₂, pH 7.4. Afterward, the slices were washed three times (5 min each) with ACSF, and fixed at room temperature with 4% PFA for 60 min, rinsed once with 0.1 mM glycine in phosphate buffered saline (PBS) for 5 min and then twice with PBS for 10 min with gentle agitation. Then, the slices were incubated two times for 30 min each with a blocking solution (PBS, gelatin 0.2%, Triton-X 100 1%) at room temperature. Afterward, the slices were incubated overnight at 4 °C with anti-GFAP monoclonal antibody (1:500, Sigma) to detect astrocytes. Later, the slices were washed three times (10 min each) with blocking solution and then incubated for 2 hr at room temperature with goat anti-mouse Alexa Fluor 488 (1:1000) antibody and DAPI. Furthermore, the slices were washed three times (10 min each) in PBS and then mounted in Fluoromount, cover-slipped and examined in a confocal laser-scanning microscope (TBCS SP2, Nikon, Japan). Stacks of consecutive confocal images were taken with \times 40 objective at 100 nm intervals were acquired sequentially with three lasers (in nm: 408, 488, and 543), and Z projections were reconstructed using Nikon confocal software (NIS-elements) and ImageJ software. Dye uptake was calculated with the following formula: Corrected total cell Etd fluorescence = Integrated Density - ([Area of selected cell] \times [Mean fluorescence of background readings]). At least six cells per field were selected from at least three fields in each brainstem slice.

2.16 | Data analysis and statistics

Detailed statistical results were included in the figure legends. Statistical analyses were performed using GraphPad Prism (version 7, GraphPad Software, La Jolla, CA). Normality and equal variances were assessed by the Shapiro-Wilk normality test and Brown-Forsythe test, respectively. Unless otherwise stated, data that passed these tests were analyzed by unpaired *t* test in case of comparing two groups, whereas in case of multiple comparisons, data were analyzed by one or two-way analysis of variance (ANOVA) followed, in case of significance, by a Tukey's post hoc test. A probability of *p* < .05 was considered statistically significant.

3 | RESULTS

3.1 | α -Synuclein enhances the activity of Cx43 hemichannels and Panx1 channels in astrocytes

Neuropathological agents, including cytokines, amyloid- β peptide (A β), and lipopolysaccharide (LPS) cause a prominent opening of hemichannels and pannexons in diverse brain cell types (Abudara et al., 2015;

Avendano et al., 2015; Orellana et al., 2011; Retamal et al., 2007; Takeuchi et al., 2006). Given that α -synuclein induces reactive astrogliosis (Fellner et al., 2013; Klegeris et al., 2006; Koob et al., 2010) and because hemichannels and pannexons may contribute to this process (Avendano et al., 2015; Karpuk, Burkovetskaya, Fritz, Angle, & Kielian, 2011; Orellana et al., 2010; Saez et al., 2013; Santiago et al., 2011; Yi et al., 2016), we examined whether α -synuclein could modulate the activity of these channels in primary cortical astrocytes. The functional state of hemichannels was evaluated by measuring the rate of Etd uptake. This dye enters the cytoplasm of healthy cells through plasma membrane channels with large pores, including hemichannels and pannexons (Johnson et al., 2016). After its intercalation with base pairs of DNA and RNA, Etd becomes fluorescent, reflecting the activity of channels when appropriate blockers are used.

We examined Etd uptake in astrocytes treated for different periods with 10 nM α -synuclein incubated or "aged" for 0, 7, or 21 days at 37 °C (see Section 2), as the aging state of this protein generates distinct effects on glial cell function (Diogenes et al., 2012; Fellner et al., 2013; Zhang et al., 2005). After treatment with nonaged α -synuclein, Etd uptake in astrocytes was almost unchanged relative to control conditions in the time intervals studied (Figure 1a). However, 7-day-old α -synuclein induced a rapid rise in astrocyte Etd uptake that peaked a 3.2-fold augmentation following 24 hr of treatment and progressively decreased in further days (Figure 1a–e). Moreover, the treatment for 24 hr with 7-day-old α -synuclein was dependent on its concentration, reaching a maximum with a 10 nM treatment. (Figure 1a,b). Because 21-day-old α -synuclein increased Etd uptake to an intermediate degree (Figure 1a), we used the 7-day-old α -synuclein (10 nM) treatment in all further experiments.

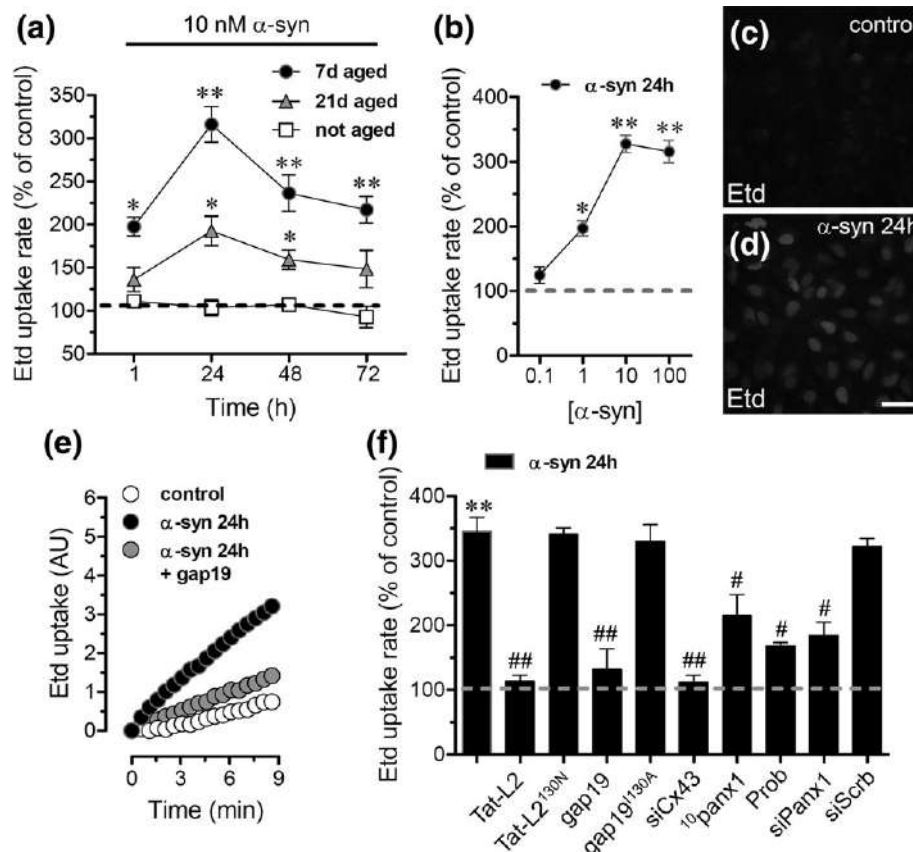


FIGURE 1 α -Synuclein increases the activity of Cx43 hemichannels and Panx1 channels in astrocytes. (a) Averaged Etd uptake rate normalized with control condition (dashed line) by astrocytes treated for several time periods with 10 nM α -synuclein not aged (white squares) or aged by 7 (black circles) or 21 (gray triangles) days. * p < .005, ** p < .0001, α -synuclein treatment compared to control conditions (two-way ANOVA followed by Tukey's post hoc test). (b) Averaged Etd uptake rate normalized with control condition (dashed line) by astrocytes treated for 24 hr with different concentrations of α -synuclein aged for 7 days (black circles). * p < .005, ** p < .0001, α -synuclein treatment compared to control conditions (one-way ANOVA followed by Tukey's post hoc test). (c,d) Representative immunofluorescence images depicting Etd staining from dye uptake measurements (10 min exposure to Etd) in astrocytes under control conditions (c) or treated for 24 hr with 10 nM α -synuclein aged for 7 days (d). (e) Time-lapse measurements of Etd uptake by astrocytes under control conditions (white circles) or treated for 24 hr with 10 nM α -synuclein aged for 7 days alone (black circles) or in combination with 100 μ M gap19 (gray circles). (f) Averaged Etd uptake rate normalized with control condition (dashed line) by astrocytes treated for 24 hr with 10 nM α -synuclein aged for 7 days alone or in combination with the following blockers: 100 μ M Tat-L2, 100 μ M Tat-L2^{H126K/I130N}, 100 μ M gap19, 100 μ M gap19^{I130A}, siRNA^{Cx43}, 100 μ M ¹⁰panx1, 500 μ M Probenecid (Prob), siRNA^{Panx1}; and siRNA^{scrb}. ** p < .0001, α -synuclein compared to control; # p < .0001, ## p < .005; effect of pharmacological agents compared to α -synuclein treatment (one-way ANOVA followed by Tukey's post hoc test). Data were obtained from at least three independent experiments with three or more repeats each one (\geq 30 cells analyzed for each repeat). Calibration bar = 20 μ m

Because Cx43 hemichannels and Panx1 channels are major pathways for dye influx in astrocytes (Iglesias et al., 2009; Retamal, Cortes, Reuss, Bennett, & Saez, 2006), the possible involvement of these channels in the α -synuclein-induced astroglial Etd uptake was studied. To do that, astrocyte cultures were preincubated for 15 min before and during Etd uptake experiments with different pharmacological agents, Tat-L2 (100 μ M) and gap19 (100 μ M). Two mimetic peptides that block Cx43 hemichannels by interacting with the intracellular L2 loop of Cx43 (Abudara et al., 2014; Ponsaerts et al., 2010; Wang et al., 2013); fully reduced α -synuclein-induced Etd uptake in astrocytes to ~113% and ~131% compared to 100% control level, respectively (Figure 1f). In addition, a modified Tat-L2 (Tat-L2^{H126K/I130N}), in which 2 aa critical for binding of L2 to the CT tail of Cx43 are mutated, failed in cause an equivalent inhibitory effect (Figure 1a). Likewise, we observed that an inactive form of gap19 containing the I130A modification (gap19I130A), did not counteract the α -synuclein-mediated Etd uptake in astrocytes (Figure 1f). Consistent with this evidence, knockdown of Cx43 with siRNA, but not the scrambled siRNA, fully abolished the Etd uptake caused by α -synuclein (Figure 1f). To scrutinize the contribution of Panx1 channels to the α -synuclein-induced Etd uptake in astrocytes, we used the mimetic peptide ¹⁰panx1 with an amino acid sequence homologous to the first extracellular loop domain of Panx1 (Pelegri & Surprenant, 2006), as well as probenecid and siRNA^{Panx1}. ¹⁰panx1 (100 μ M), probenecid (500 μ M) and downregulation of Panx1 partially blunted the α -synuclein-mediated astrocyte Etd uptake (Figure 1f). These findings substantially indicate that α -synuclein treatment increases the opening of Cx43 hemichannels and Panx1 channels in astrocytes.

3.2 | α -Synuclein-induced hemichannel and pannexon activity depends on cytokine production and activation of p38 MAPK/iNOS/COX₂/[Ca²⁺]_i-dependent pathways and purinergic/glutamatergic signaling

Given that prior studies have revealed the involvement of TNF- α /IL-1 β , p38 MAPK, iNOS/NO, COXs, EP₁ receptor, and cytoplasmic Ca²⁺ in the opening of glial cell hemichannels and pannexons (Avendano et al., 2015; De Bock et al., 2012; Gajardo-Gomez et al., 2017; Retamal et al., 2007), we tested whether these factors were also implicated in the α -synuclein-induced Cx43 hemichannel and Panx1 channel activity in astrocytes. Pretreatment with a soluble form of TNF- α receptor that binds TNF- α (sTNF-aR1) and a recombinant antagonist for the IL-1 β receptor (IL-1ra) dramatically inhibited the Etd uptake evoked by α -synuclein (Figure 2). When sTNF-aR1 or IL-1ra were applied by themselves, also a significant but partial counteracting effect was detected (Figure 2). Similarly, the α -synuclein-mediated Etd uptake in astrocytes was strongly blunted by inhibition of p38 MAPK with 1 μ M SB202190 or blockade of iNOS with 5 μ M L-N6 (Figure 2). Notably, ns-398 (5 μ M), a COX₂ blocker, dramatically neutralized the Etd uptake caused by α -synuclein, whereas sc-560 (20 nM), a COX₁ inhibitor, failed to produce a similar response (Figure 2).

NO increases COX₂ activity and prostaglandin E₂ (PEG₂) generation in macrophages (Swierkosz, Mitchell, Warner, Botting, & Vane, 1995) and a similar effect likely takes place in astrocytes treated with α -synuclein (Yu et al., 2018). Because stimulation of PEG₂ receptor 1 (EP₁) triggers the rise of intracellular free Ca²⁺ concentration ([Ca²⁺]_i) and the latter is a well-recognized mechanism that enhances the open probability of Cx43 hemichannels (De Bock et al., 2012) and Panx1 channels (Locovei, Wang, & Dahl, 2006), we explored whether this pathway was associated with the α -synuclein-induced Etd uptake in astrocytes. Inhibition of the EP₁ receptor with sc-19220 (20 μ M) did not affect the Etd uptake caused by α -synuclein, whereas 5 μ M BAPTA-AM, a Ca²⁺ chelator, triggered a partial blockade (Figure 2).

The opening of Cx43 hemichannels and Panx1 channels has been correlated with [Ca²⁺]_i-mediated purinergic (Baroja-Mazo, Barbera-Cremades, & Pelegri, 2013; Chi et al., 2014) and glutamatergic signaling (Voigt et al., 2015; Weilinger, Tang, & Thompson, 2012), thereby, we evaluated if these pathways contribute to the α -synuclein-dependent Etd uptake in astrocytes. Noteworthy, 200 μ M oATP, a wide-spectrum P2X receptor blocker, or 200 nM A740003, a P2X₇ receptor antagonist, partially inhibited the Etd uptake induced by α -synuclein (Figure 2). In a like manner, the suppression of P2Y₁ receptors with 1 μ M MRS2179 triggered a partial but significant decrease in the α -synuclein-mediated Etd uptake (Figure 2). On the other hand, 1 μ M 2-AP5 or 1 μ M CPP, two selective NMDA receptor antagonists, but not the selective mGluR_{2/3} antagonist LY341495 (200 nM), caused a partial reduction in the Etd uptake induced by α -synuclein. The pattern of Etd uptake inhibition evoked by some of these antagonists was similar to that found in astrocytes stimulated with α -synuclein and Panx1 channel inhibitors (Figure 1f and 2). This leads us to think that Panx1 channel opening could occur downstream or with a positive feedback loop related to the activation of purinergic/glutamatergic signaling. Supporting this idea, the Panx1 channel blocker probenecid did not elicit any additive inhibition in the α -synuclein-induced Etd uptake when astrocytes were treated with BAPTA, oATP, A740003, MRS2179, 2-AP5, or CPP (Figure 2). Collectively, these findings suggest that astrocyte Cx43 hemichannel and Panx1 channel activity triggered by α -synuclein differentially depend on the stimulation of p38 MAPK/iNOS/COX₂-dependent pathway(s), as well as P2X₇/P2Y₁/NMDA receptors and rise on [Ca²⁺]_i.

3.3 | α -Synuclein reduces astrocyte-to-astrocyte communication and alters the amount and distribution of Panx1 but not Cx43

Astrocyte coupling via gap junctions determines the propagation of intercellular Ca²⁺ waves and spatial buffering of neurotransmitters, K⁺ and H⁺, thus sculpting an extracellular environment that ensures proper neuronal function (De Bock et al., 2014). Because the increased opening of hemichannels and pannexons may take place in parallel with astroglial uncoupling (Avendano et al., 2015; Gajardo-Gomez et al., 2017; Retamal et al., 2007), we explored whether the

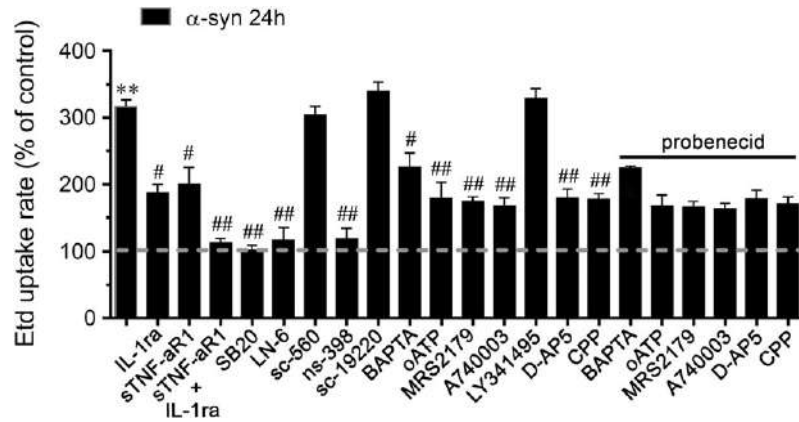


FIGURE 2 The α -synuclein-induced Cx43 hemichannel and Panx1 channel activity depend on proinflammatory cytokines and activation of p38 MAPK/iNOS/COX₂/[Ca²⁺]_i-dependent pathways and purinergic/glutamatergic signaling. Averaged Etd uptake rate normalized with control condition (dashed line) by astrocytes treated for 24 hr with 10 nM α -synuclein alone or in combination with the following agents: 100 ng/mL of IL-1ra, 100 ng/mL of sTNF- α R1, 100 ng/mL of IL-1ra + 100 ng/mL of sTNF- α R1, 1 μ M SB203580, 1 μ M L-N6, 20 nM sc-560; 5 μ M ns-398; 20 μ M sc-19220, 10 μ M BAPTA, 200 μ M oxidized ATP (oATP), 1 μ M MRS2179; 200 nM A740003, 100 nM LY341495; 1 μ M D-AP5 or 1 μ M CPP. It is also shown the effect of 24 hr with 10 nM α -synuclein plus 500 μ M probenecid alone or in combination with the following agents: 10 μ M BAPTA, 200 μ M oxidized ATP (oATP), 1 μ M MRS2179; 200 nM A740003, 1 μ M D-AP5 or 1 μ M CPP. ** p < .0001, α -synuclein treatment compared to control conditions; # p < .0001, ## p < .005; effect of pharmacological agents compared to α -synuclein treatment; $^{\$}$ p < .05, effect of probenecid compared to α -synuclein treatment plus pharmacological agents (one-way ANOVA followed by Tukey's post hoc test). Data were obtained from at least three independent experiments with three or more repeats each one (\geq 30 cells analyzed for each repeat)

functional state of astroglial gap junctions is disturbed by α -synuclein. Similar to prior studies (Avendano et al., 2015), control astrocytes display a strong intercellular coupling to LY (Figure 3a). However, the stimulation of astrocytes with α -synuclein for 24 hr notoriously blunted the intercellular LY transfer by ~50% compared to control values (Figure 3a–c). Given that internalization of gap junctions from the plasma membrane is a phenomenon that might result in cellular uncoupling, we examined whether α -synuclein-mediated astroglial uncoupling was linked to alterations in the distribution of Cx43 in confluent astrocytes. Under control conditions, Cx43 was observed as fine to large granules scattered at cellular interfaces (Figure 3d,e) and comparable patterns were detected in astrocytes treated with α -synuclein for 24 h (Figure 3f–g). These results suggest that α -synuclein-induced astrocyte-to-astrocyte uncoupling bases in a mechanism implicating the closure and/or reduced permeability of gap junctions rather than endocytosis from the cell–cell interfaces.

The activity of hemichannels and pannexons could rely on arguments in the open probability per channel, conductance/selectivity and/or the number of channels at the plasma membrane. Prior evidence has linked the channel-dependent Etd uptake with increased surface levels of Cx43 and Panx1 in different cell types (Avendano et al., 2015; Gajardo-Gomez et al., 2017) or increase in open probability without changes in the total amount of Cx43 in the cell surface (Schalper et al., 2008). Here, we evaluated whether the α -synuclein-mediated Etd uptake correlates with changes in total and/or surface amount of Cx43 and Panx1. Western blot analysis revealed that stimulation with α -synuclein did not change total levels of Cx43 in astrocytes (Figure 4a,b). However, α -synuclein caused a significant ~60%

and ~55% reduction in total levels of Panx1 after 24 and 48 hr of treatment, respectively (Figure 4a,c).

Because gap junctional communication depends on the phosphorylation state of connexins (Lampe & Lau, 2004), we decided to study whether α -synuclein affects this parameter. Phosphorylation of Cx43 affects its electrophoretic mobility when analyzed by SDS-PAGE, which result in multiple isoforms including a faster migrating nonphosphorylated (NP) form of Cx43, and at least two slower migrating phosphorylated forms, usually termed P1 and P2 (Crow, Beyer, Paul, Kobe, & Lau, 1990). Control astrocytes exhibited three bands with electrophoretic mobilities equivalent to the NP, P2, and P1 forms of Cx43 (Figure 4a). After treatment with α -synuclein, the intensity and band pattern (NP, P1, and P2 forms) of Cx43 were indistinguishable from control conditions (Figure 4a,d). This result suggests that α -synuclein does not alter the phosphorylation state of Cx43 as preliminarily measured by changes in its electrophoretic mobility. Nevertheless, it is also important to note that changes in phosphorylation of Cx43 not necessarily cause a shift in its electrophoretic mobility (Solan & Lampe, 2009). Therefore, to scrutinize deeper in this matter, we used an antibody to detect the phosphorylation of Cx43 at serine 368 (S368), a residue crucial for the PKC-mediated reduction in gap junction channel conductance and selectivity (Ek-Vitorin, King, Heyman, Lampe, & Burt, 2006; Lampe et al., 2000). Densitometric analysis revealed that 24 hr of treatment with α -synuclein does not modify the phosphorylation levels of Cx43 at serine 368 compared to control conditions (Figure 4e,f), indicating that this phosphorylation is not required for the α -synuclein-induced reduction of intercellular LY transfer between astrocytes.

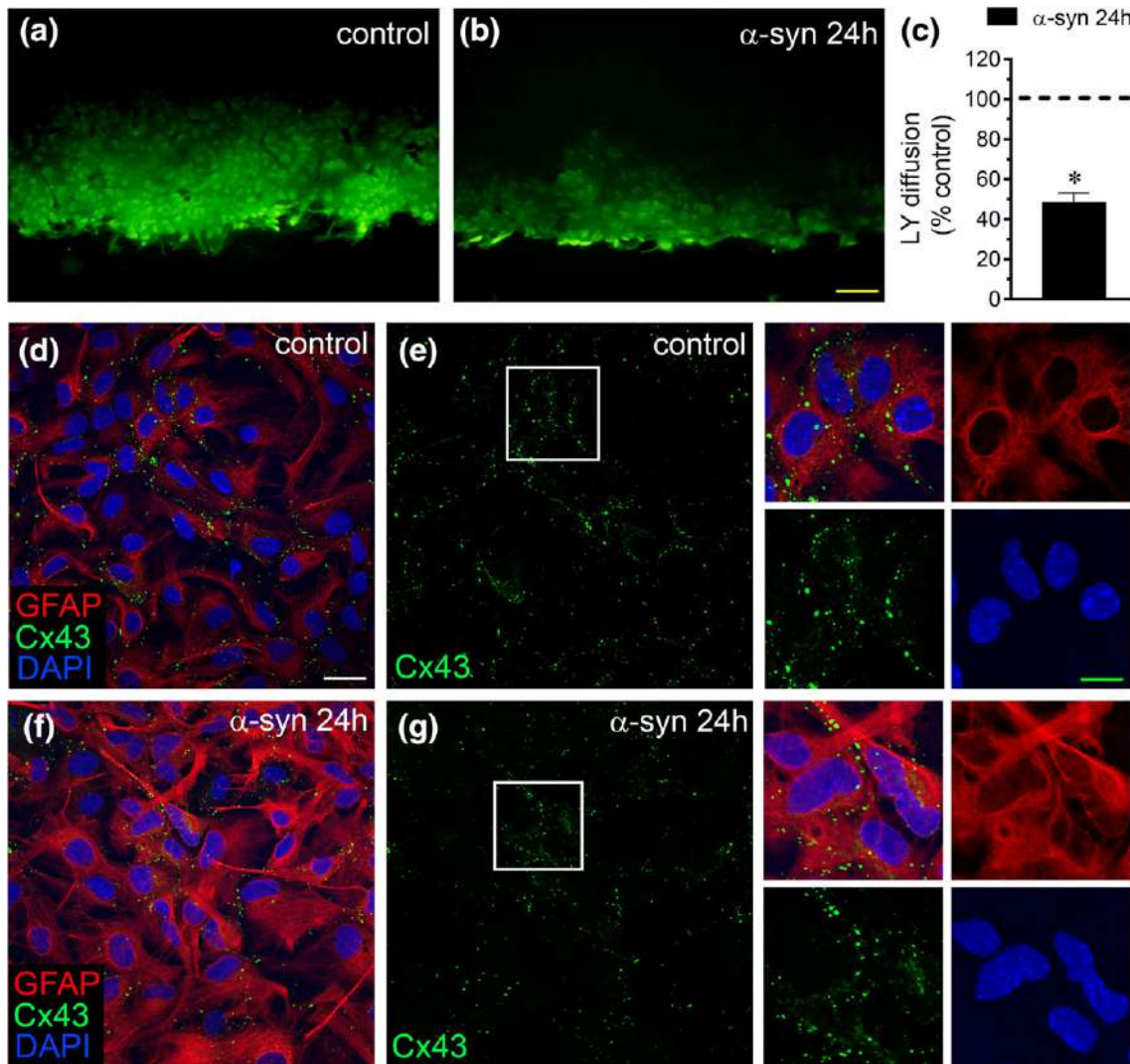


FIGURE 3 α -Synuclein decreases astroglial coupling by a mechanism that does not involve changes in Cx43 distribution. (a,b) Representative fluorescence micrographs of SL/DT with LY by astrocytes under control conditions (a) or treated for 24 hr with 10 nM α -synuclein (b). (c) Averaged data normalized to control (dashed line) of SL/DT with LY by astrocytes treated for 24 hr with 10 nM α -synuclein. * $p < .05$, α -synuclein treatment compared to control conditions (two-tailed Student's unpaired t test). Data were obtained from at least three independent experiments with three or more repeats each one. Yellow calibration bar = 250 μ m. (d-g) Representative fluorescence images depicting Cx43 (green), GFAP (red), and DAPI (blue) staining by astrocytes under control conditions (d,e) or treated for 24 hr with 10 nM α -synuclein (f,g). Insets: $\times 2.5$ magnification of the indicated area of panels e and g. calibration bars: White = 80 μ m and green = 35 μ m [Color figure can be viewed at wileyonlinelibrary.com]

In complementary studies, we used confocal microscopy to evaluate the distribution of Cx43 and Panx1 in subconfluent astrocytes, the latter being a strategy to mostly detect the surface Cx43 in the form of hemichannels rather than gap junction channels. Colocalization analysis with the membrane marker wheat germ agglutinin (WGA) revealed that surface, intracellular and total levels of Cx43 remains unaltered after stimulating astrocytes with α -synuclein for 24 hr (Figure 5a–f and m). In parallel experiments, the treatment with α -synuclein for 24 hr was found to decrease in 25% the intracellular levels of Panx1 in astrocytes without changing its surface levels (Figure 5g–l and n). These results implicate that Cx43 hemichannel and Panx1 channel activity triggered by

α -synuclein likely does not occur by changes in the number of channels in the plasma membrane.

3.4 | The α -synuclein-mediated release of gliotransmitters depends on the opening of astroglial Cx43 hemichannels and Panx1 channels

Scenarios of inflammation often cause an increased hemichannel and/or pannexon-dependent release of glutamate and ATP from astrocytes (Avendano et al., 2015; Gajardo-Gomez et al., 2017; Orellana et al., 2011). Given that glutamatergic and purinergic signaling participates in the opening of astroglial hemichannels and

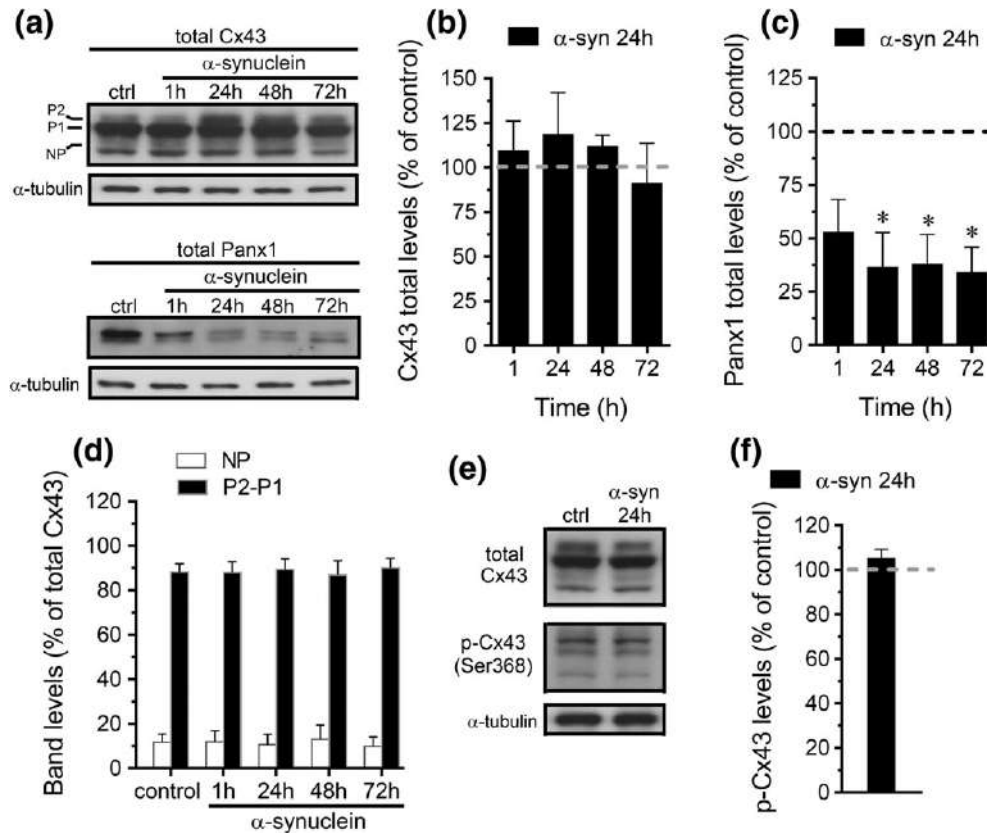


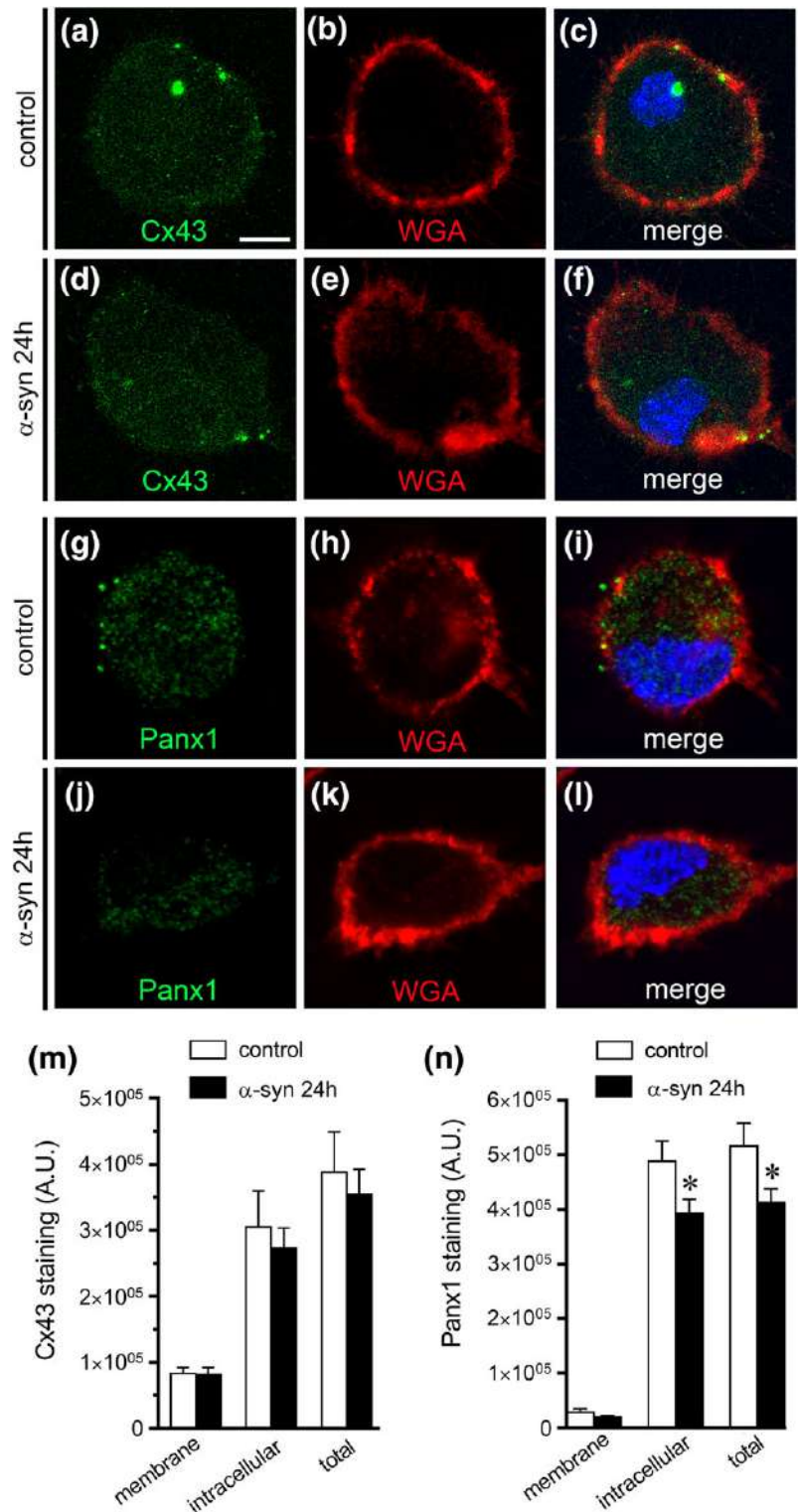
FIGURE 4 α -Synuclein decreases total levels of Panx1 but not alter total levels neither phosphorylation at ser368 of Cx43 in astrocytes. (a) Total levels of Cx43 (upper panel) and Panx1 (bottom panel) by astrocytes under control conditions or treated for 1, 24, 48, or 72 hr with 10 nM α -synuclein. The Cx43 phosphorylated (P1–P2) and nonphosphorylated (NP) forms are indicated in the left. Total levels of each analyzed band were normalized according to the levels of α -tubulin detected in each lane. (b,c) quantification of total levels of Cx43 (b) and Panx1 (c) normalized to control (dashed line) in astrocytes treated for 1, 24, 48, or 72 hr with 10 nM α -synuclein. $**p < .0001$, α -synuclein treatment compared to control conditions. (e) Total (upper panel) and phosphorylated (middle panel) levels of Cx43 at ser368 by astrocytes under control conditions (left) or treated for 24 hr with 10 nM α -synuclein (right). Phosphorylated levels of each analyzed band were normalized according to the levels of α -tubulin in each lane. (f) Quantification of phosphorylated levels of Cx43 at ser368 normalized to control (dashed line) in astrocytes for 24 hr with 10 nM α -synuclein. Averaged data were obtained from three independent experiments

pannexons (Iglesias et al., 2009; Orellana et al., 2014, 2015), we evaluated whether α -synuclein affects the release of glutamate and ATP from astrocytes. Treatment with α -synuclein for 24 hr dramatically augmented the release of glutamate and ATP in ~ninefold and ~sixfold compared to control conditions (Figure 6a,b). Importantly, Tat-L2 or gap19, but not 10 panx1 or probenecid, prominently blunted the release of glutamate caused by α -synuclein (from ~126 pmol/mg to ~18 pmol/mg and ~16 pmol/mg, respectively; Figure 6a). In agreement with this, knockdown of Cx43 with siRNA, but not the Panx1 or scrambled siRNA, fully abolished the release of glutamate caused by α -synuclein (Figure 6a). At the other end, Tat-L2, gap19, 10 panx1, or probenecid, strongly reduced to control values the α -synuclein-induced release of ATP (from ~112 pmol/mg to ~31 pmol/mg, ~30 pmol/mg, ~33 pmol/mg and ~28 pmol/mg, respectively; Figure 6b). Consistent with the above evidence, knockdown of Cx43 or Panx1, but not the scrambled siRNA, totally abrogated the release of ATP caused by α -synuclein (Figure 6b).

The different contribution of Cx43 hemichannels and Panx1 channels to the α -synuclein-induced release of glutamate versus ATP

(Figure 6a,b) could imply that ATP release may occur downstream to the release of glutamate following the activation of glutamatergic signaling. Supporting this idea, the NMDA receptor antagonists 2-AP5 or CPP totally inhibited the α -synuclein-induced release of ATP but not of glutamate (Figure 6a,b). The fact that α -synuclein-mediated opening of Panx1 channels was associated with the activation of NMDA and P2X₇/P2Y₁ receptors (Figure 2) may suggest that ATP release takes place by an NMDA-dependent stimulation of Panx1 channels and the subsequent positive feed-forward loop of purinergic signaling. In this line, oATP, A740003, or MRS2179 significantly blocked the α -synuclein-evoked release of ATP (Figure 6b). In contrast, the release of glutamate triggered by α -synuclein was not altered by oATP, A740003, or MRS2179, suggesting that P2X₇/P2Y₁ receptor-dependent release of ATP likely occurs downstream to the release of glutamate (Figure 6a). The latter transmitter likely is released by the activation of Cx43 hemichannels as the release of both ATP and glutamate were completely abolished by inhibitions of these channels (Figure 6a,b). Relevantly, in agreement with the fact that Cx43 hemichannels or Panx1 channels are activated by cytoplasmic Ca²⁺

FIGURE 5 α -Synuclein decreases intracellular levels of Panx1 but does not alter surface levels of Panx1 and Cx43 in astrocytes. (a–f) Representative confocal images depicting Cx43 (green), WGA (red), and Hoechst (blue) staining by astrocytes under control conditions (a–c) or treated for 24 hr with 10 nM α -synuclein (d–f). (g–l) Representative confocal images depicting Panx1 (green), WGA (red), and Hoechst (blue) staining by astrocytes under control conditions (g–i) or treated for 24 hr with 10 nM α -synuclein (j–l). Calibration Bar: 10 μ m. (m,n) Quantification of membrane, intracellular, and total staining of Cx43 (m) and Panx1 (n) by astrocytes under control conditions (white bars) or treated for 24 hr with 10 nM α -synuclein (black bars). * $p < .05$, α -synuclein treatment compared to control conditions (two-tailed Student's unpaired t test). Data were obtained from at least three independent experiments with three or more repeats each one (≥ 20 cells analyzed for each repeat) [Color figure can be viewed at wileyonlinelibrary.com]



(De Bock et al., 2012; Locovei et al., 2006), BAPTA partially blunted the α -synuclein-induced release of both glutamate and ATP (Figure 6a,b). Altogether these observations imply that α -synuclein triggers the release of glutamate and ATP in astrocytes by a mechanism that requires the activation of a complex variety of membrane channels and receptors, including Cx43 hemichannels, NMDA receptors, Panx1 channels, and P2X₇/P2Y₁ receptors.

3.5 | The α -synuclein-induced production of NO and altered mitochondrial morphology depends on the opening of Cx43 hemichannels and Panx1 channels in astrocytes

During neuropathological conditions, astrocytes may release large amounts of proinflammatory cytokines, whose autocrine/paracrine

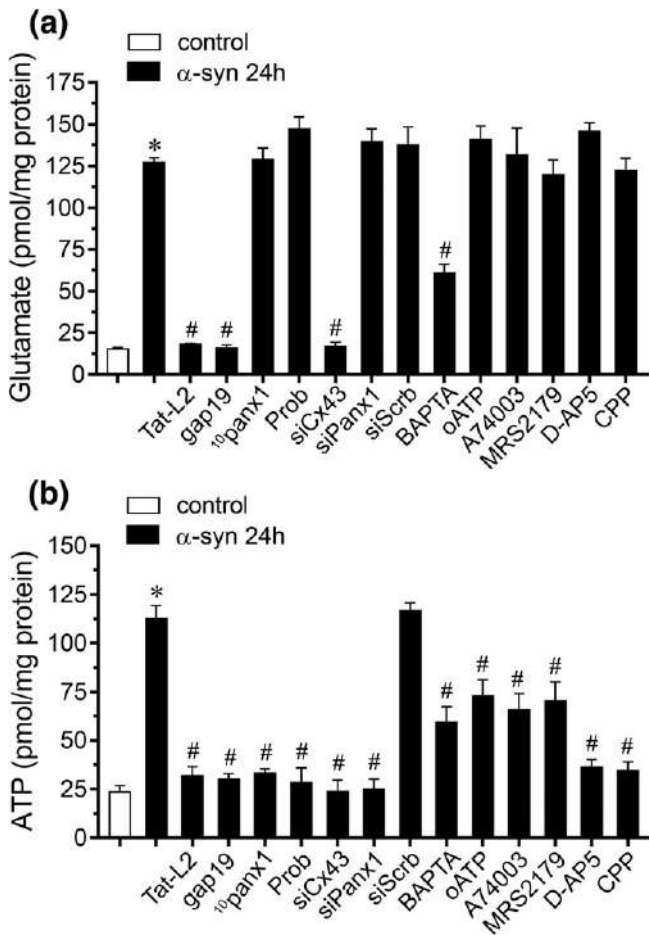


FIGURE 6 α -Synuclein increases the release of gliotransmitters via the opening of Cx43 hemichannels and Panx1 channels. Averaged data of glutamate (a) or ATP (b) release by astrocytes under control conditions (white bars) or treated for 24 hr with 10 nM α -synuclein alone (black bars) or in combination with the following agents: 100 μ M Tat-L2, 100 μ M gap19, 100 μ M 10 panx1, 500 μ M Probenecid (Prob), siRNA^{Cx43}, siRNA^{Panx1}, siRNA^{scrib}, 10 μ M BAPTA, 200 μ M oxidized ATP (oATP), 200 nM A740003, 1 μ M MRS2179; 1 μ M D-AP5 or 1 μ M CPP. * $p < .0001$, α -synuclein treatment compared to control conditions; # $p < .0001$, effect of pharmacological agents compared to α -synuclein treatment (one-way ANOVA followed by Dunnett's post hoc test). Data were obtained from at least three independent experiments with three or more repeats each one

signaling could impact astrocyte homeostasis at the molecular, morphological, and functional level (Agulhon et al., 2012). In this line, the opening of Cx43 hemichannels in astrocytes has been observed upon the treatment with IL-1 β and TNF- α (Abudara et al., 2015; Retamal et al., 2007). Because sTNF-r1 and IL-1ra greatly abrogated the α -synuclein-induced Etd uptake by astrocytes (Figure 2), we explored if α -synuclein could disturb the release of IL-1 β and TNF- α in our system. Upon 24 hr of stimulation with α -synuclein, astrocytes showed a ~eightfold and ~10-fold augment in the release of IL-1 β and TNF- α compared with control levels, respectively (Figure 7a,b). Of note, astrocytes treated for 24 with these concentrations of IL-1 β (2 ng/mL) and TNF- α (1 ng/mL) exhibited values of Etd uptake indistinguishable from those triggered by α -synuclein (Figure S51). Previous studies have

related the opening of hemichannels and pannexons with the production and release of cytokines in diverse cell types (Mugisho et al., 2018; Parzych et al., 2017; Pelegrin & Surprenant, 2006), including astrocytes (Wei et al., 2016). In contrast to this evidence, we found that Tat-L2, gap19 or 10 panx1 failed in to prevent the α -synuclein-induced release of IL-1 β and TNF- α , suggesting that Cx43 hemichannels and Panx1 channels are not implicated in this response.

During reactive astrogliosis, the activation of iNOS is one of the major downstream targets of IL-1 β /TNF- α signaling (Agulhon et al., 2012). Because LN-6, a specific iNOS inhibitor, strongly counteracted the α -synuclein-mediated Etd uptake in astrocytes (Figure 2), we investigated if α -synuclein could impact the production of NO in these cells. DAF-FM fluorescence imaging showed that α -synuclein-treated astrocytes exhibit a ~twofold increase in basal NO levels compared to those under control conditions (Figure 7c,d and h,i). Of note, Tat-L2, gap19, or 10 panx1 completely suppressed the production of NO caused by α -synuclein in astrocytes (from ~203% to ~80%, ~102% or ~88%, compared to 100% of control, respectively), revealing that Cx43 hemichannels and Panx1 channels are crucial for this phenomenon (Figure 7c,f,g,j,k).

Stimulation of iNOS and further production of NO disturb the function and morphology of astrocyte mitochondria (Motori et al., 2013). In this context and given that α -synuclein induces mitochondrial fragmentation in astrocytes (Fellner et al., 2013; Gustafsson et al., 2017; Lindstrom et al., 2017), we examined whether this protein could modify mitochondrial morphology of astrocytes by a mechanism involving the activation of Cx43 hemichannels and/or Panx1 channels. To do that, we measured the size of mitochondria by using the fluorescent probe MitoTracker Green. Astrocytes stimulated with α -synuclein for 24 hr exhibited smaller mitochondria (~35% size reduction) compared to control conditions (Figure 7l-n). Similar to that found for NO production, gap19 greatly blunted the reduction in mitochondrial size evoked by α -synuclein in astrocytes (from ~4.6 μ m to ~6.2 μ m; Figure 7l). In addition, 10 panx1 also slightly prevented the α -synuclein-induced reduction in mitochondrial size (from ~4.6 μ m to ~5.1 μ m, Figure 7l), suggesting that Cx43 hemichannels and Panx1 channels are involved in this response.

3.6 | α -Synuclein alters ATP-mediated [Ca²⁺]_i dynamics by a mechanism that involve the opening of Cx43 hemichannels and Panx1 channels in astrocytes

Moderate increments (>500 nM) in [Ca²⁺]_i cause the opening of Cx43 hemichannels (De Bock et al., 2012), whereas equivalent responses seem to take place with Panx1 channels (Locovei et al., 2006). Moreover, [Ca²⁺]_i dynamics control astroglial activation and function, as well as the release of gliotransmitters through different pathways (Volterra et al., 2014), including those associated with the opening of Cx43 hemichannels (Meunier et al., 2017). Because BAPTA significantly blocked the α -synuclein-induced Etd uptake by astrocytes, we tested whether α -synuclein could alter [Ca²⁺]_i levels in these cells. As depicted by the measure of Fura-2AM ratio (340/380), astrocytes

treated for 1, 24, 48, or 72 hr with α -synuclein displayed basal Ca^{2+} levels that were similar to those under control conditions (Figure 8a,c,g).

Although α -synuclein did not affect the basal Ca^{2+} signal, these findings do not rule out whether α -synuclein modulates Ca^{2+} dynamics triggered by autocrine/paracrine gliotransmitters, such as ATP. Given that this gliotransmitter is released through Cx43 hemichannels and Panx1 channels upon treatment with α -synuclein (Figure 6a), we also explored the impact of this condition on ATP-mediated Ca^{2+} signaling.

After treatment with 500 μM ATP, control astrocytes exhibited a rapid Ca^{2+} signal response with a large peak amplitude (Figure 8b,e,h). Nevertheless, astrocytes stimulated with α -synuclein showed a time-dependent reduction in the Ca^{2+} peak response that reached a maximum decrease of \sim twofold following 48 hr of treatment (Figure 8d,f,h). This phenomenon was accompanied by a time-dependent decrease in the integrated ATP-dependent Ca^{2+} signal response and the remaining difference between the final and initial basal Ca^{2+} signal (Figure 8i,j).

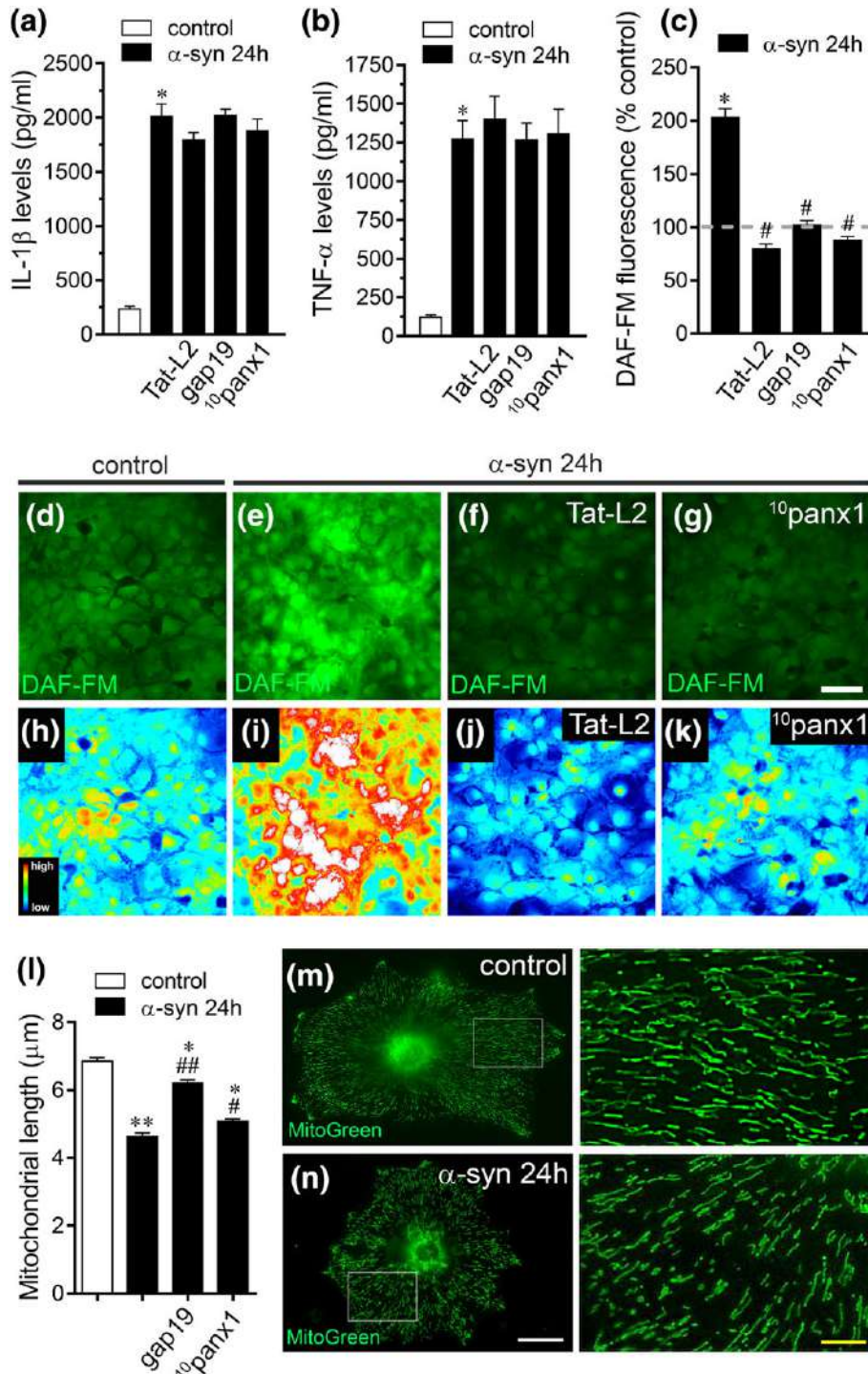


FIGURE 7 Legend on next page.

These data indicate that α -synuclein decrease ATP-mediated Ca^{2+} signaling in astrocytes.

Hemichannels and pannexons regulate $[\text{Ca}^{2+}]_i$ responses, as they are permeable to Ca^{2+} (Fiori et al., 2012; Ishikawa et al., 2011) and because they release molecules (e.g., ATP) that impact $[\text{Ca}^{2+}]_i$ dynamics (Baroja-Mazo et al., 2013). Notably, blockade of Cx43 hemichannels with Tat-L2 and gap19 totally prevented the decrease in ATP-mediated Ca^{2+} peak induced by treatment with α -synuclein for 48 hr (Figure 8k). In addition, the inhibition of Cx43 hemichannels completely blunted the reduction in the integrated and remaining basal ATP-dependent Ca^{2+} signal responses evoked by α -synuclein (Figure 8l,m). Notably, similar preventive effects on α -synuclein-induced alterations in $[\text{Ca}^{2+}]_i$ dynamics were observed upon blockade of Panx1 channels with $^{10}\text{panx1}$ (Figure 8k-m). Altogether these findings suggest that opening of Cx43 hemichannels and Panx1 channels contribute to the α -synuclein-induced decrease in ATP-mediated Ca^{2+} signaling in astrocytes.

3.7 | α -Synuclein causes astrocyte death by a mechanism involving the Cx43 hemichannel-dependent release of glutamate and further activation of mGluR₅ and AQP4 channels

Recent evidence has revealed that α -synuclein triggers astroglial death (Liu et al., 2018), whereas the uncontrolled opening of Cx43 hemichannels seems critical for inducing cell damage in astrocytes (Orellana et al., 2010; Rovigno et al., 2015). With this in mind, we assayed whether α -synuclein could mediate astrocyte death by a mechanism implicating the opening of Cx43 hemichannel and/or Panx1 channels. We examined the incorporation of EthD-1, indicative of loss of membrane integrity as due to its large size, this molecule is taken up only by cells with disrupted membranes. Under control conditions, few astrocytes took up EthD-1 (Figure 9a,j). Nevertheless, after 48 or 72 hr of treatment with α -synuclein, ~15% and ~30% of astrocytes took up EthD-1 and were dead, respectively (Figure 9b,j). Relevantly, astrocyte

death induced by 72 hr of treatment with α -synuclein was greatly prevented by the Cx43 hemichannel blocker gap19 (Figure 9c,k), whereas the Panx1 channel inhibitors $^{10}\text{panx1}$ and probenecid were slightly protective (Figure 9d,k).

Recently, it was described that the aquaporin-4 (AQP4) water channel mediates the glutamate-induced astrocyte swelling via mGluR₅ activation (Shi et al., 2017). Given that in our system α -synuclein increased the release of glutamate via the activation of Cx43 hemichannels, we examined the contribution the release of mGluR₅ and AQP4 α -synuclein-induced astrocyte death. We found that α -synuclein-evoked astrocyte death was strongly prevented by 50 nM MTEP or 5 μM SIB-1757, two selective antagonists of mGluR₅ (Figure 9e), whereas the selective NMDA receptor antagonist D-AP5 caused similar weak protection than Panx1 channel inhibitors (Figure 9e). Noteworthy, selective blockade of AQP4 with TGN-020 totally counteracted the astrocyte cell death triggered by α -synuclein (Figure 9e). Taken together these findings suggest that astroglial death resulting from α -synuclein treatment is due to the Cx43 hemichannel-dependent release of glutamate and subsequent activation of mGluR₅ and opening of AQP4 water channels.

3.8 | α -Synuclein increases the activity of Cx43 hemichannels and Panx1 channels in astrocytes of brainstem slices

To evaluate the effect of α -synuclein in a more integrated system, we investigated its influence on astrocyte hemichannels and pannexons in the brainstem, a region where α -synucleinopathies predominate (Seidel et al., 2015). Etd uptake was evaluated in "snapshot" experiments in GFAP-positive astrocytes of control brainstem slices or after treatment with 10 nM α -synuclein for 3 hr. Treatment with α -synuclein increased in ~2.6-fold the Etd uptake of astrocytes in the intermediate reticular formation of the brainstem compared to control conditions (Figure 10a-c). Similar to the preventive effect of hemichannel and pannexon inhibitors on Etd

FIGURE 7 The α -synuclein-induced release of proinflammatory cytokines is associated with increased levels of NO and alterations in mitochondrial morphology that involve the opening of Cx43 hemichannels and Panx1 channels in astrocytes. (a,b) Averaged data of levels of IL-1 β (a) and TNF- α (b) found in the extracellular media of astrocytes cultured under control conditions (white bars) or treated for 24 hr with 10 nM α -synuclein alone (black bars) or in combination with the following agents: 100 μM Tat-L2, 100 μM gap19, and 100 μM $^{10}\text{panx1}$. * p < .0001, α -synuclein treatment compared to control conditions (one-way ANOVA followed by Dunnett's post hoc test). Data were obtained from at least three independent experiments with three or more repeats each one. (c) Average of DAF-FM fluorescence normalized to control conditions (dashed line) by astrocytes treated for 24 hr with 10 nM α -synuclein alone or in combination with the following agents: 100 μM Tat-L2, 100 μM gap19 and 100 μM $^{10}\text{panx1}$. * p < .0001, α -synuclein treatment compared to control conditions, # p < .0001, effect of pharmacological agents compared to α -synuclein treatment (one-way ANOVA followed by Tukey's post hoc test). Data were obtained from at least three independent experiments with three or more repeats each one (≥ 35 cells analyzed for each repeat). (d-k) Representative fluorescence micrographs of basal NO production (DAF-FM, green and pseudo-colored scale) by astrocytes under control conditions (d-h) or treated for 24 hr with 10 nM α -synuclein alone (e-i) or in combination with 100 μM tat-L2 (f-j) or 100 μM $^{10}\text{panx1}$ (g-k). (l) Average of mitochondrial length by astrocytes under control conditions (white bar) or treated for 24 hr with 10 nM α -synuclein (black bars) alone or in combination with the following agents: 100 μM gap19 and 100 μM $^{10}\text{panx1}$. * p < .01, ** p < .001, α -synuclein treatment and effect of pharmacological agents compared to control conditions, # p < .01, ## p < .001, effect of pharmacological agents compared to α -synuclein treatment (one-way ANOVA followed by Tukey's post hoc test). Data were obtained from at least three independent experiments with three or more repeats each one (≥ 25 cells analyzed for each repeat). (m,n) Representative fluorescence micrographs of mitochondrial morphology (MitoGreen, green) by astrocytes under control conditions (m) or treated for 24 hr with 10 nM α -synuclein (n). Insets: $\times 3.5$ magnification of the indicated area of panels m and n. Calibration bars: White = 100 μm , green = 25 μm , and yellow = 6.5 μm [Color figure can be viewed at wileyonlinelibrary.com]

uptake in cultures (Figure 1f), we found that 100 μ M Tat-L2 or 100 μ M gap19 abrogated almost totally the astroglial Etd uptake evoked by α -synuclein in brainstem slices (from \sim 260% to \sim 140% or \sim 144%, compared to 100% control, respectively; Figure 10c). On the other hand, 100 μ M 10 panx1 or 500 μ M probenecid also significantly blunted the α -synuclein-induced Etd uptake by astrocytes (from \sim 260%

to \sim 204% or \sim 212%, compared to 100% control, respectively; Figure 10c). In addition, when the IL-1 β /TNF- α signaling was counteracted with sTNF-aR1 and IL-1ra, the α -synuclein-induced Etd uptake was completely abolished in brainstem astrocytes, whereas similar findings were observed upon inhibition of iNOS and COX₂ with 1 μ M LN-6 and 5 μ M ns-398, respectively (Figure 10c). The above

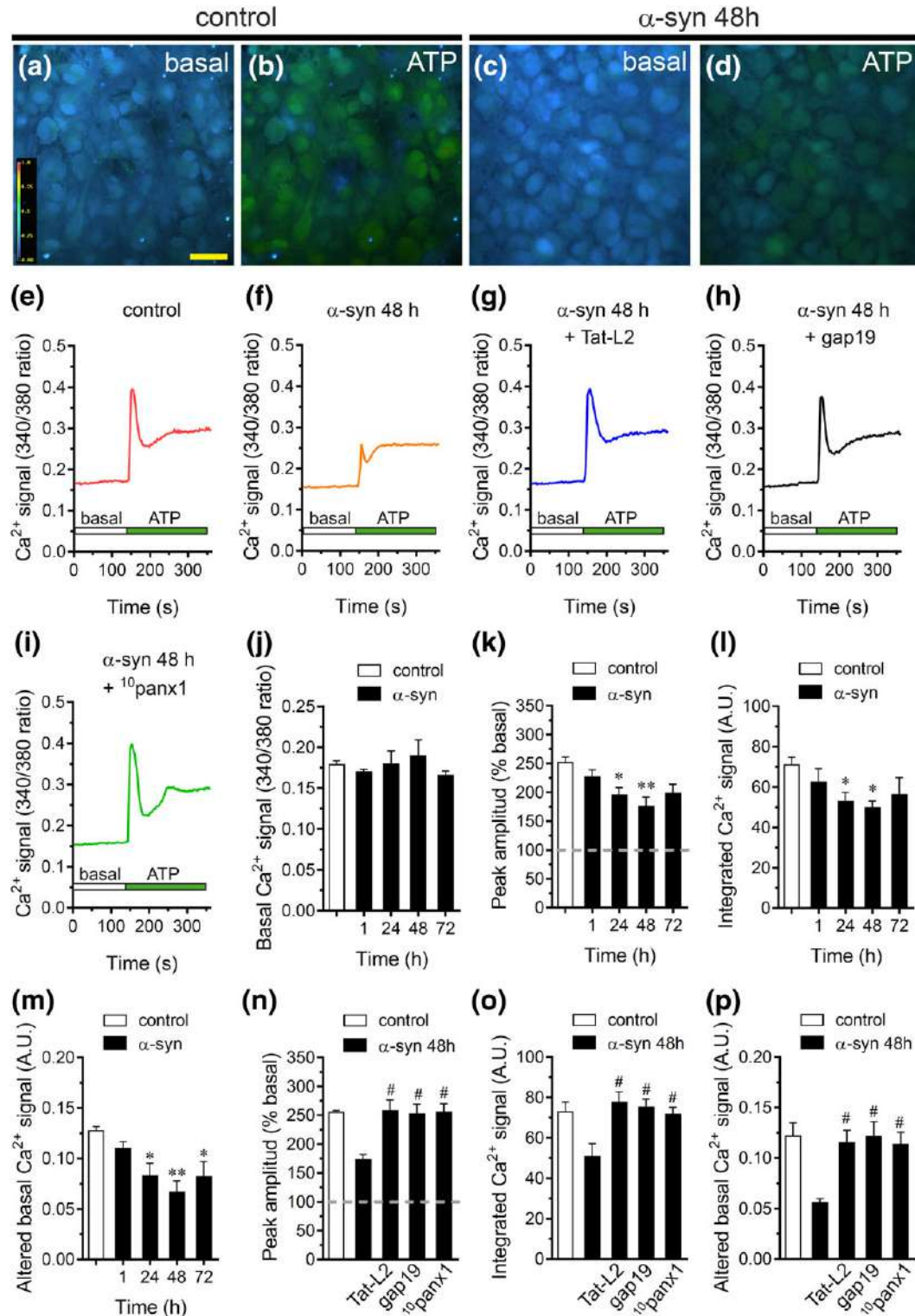


FIGURE 8 Legend on next page.

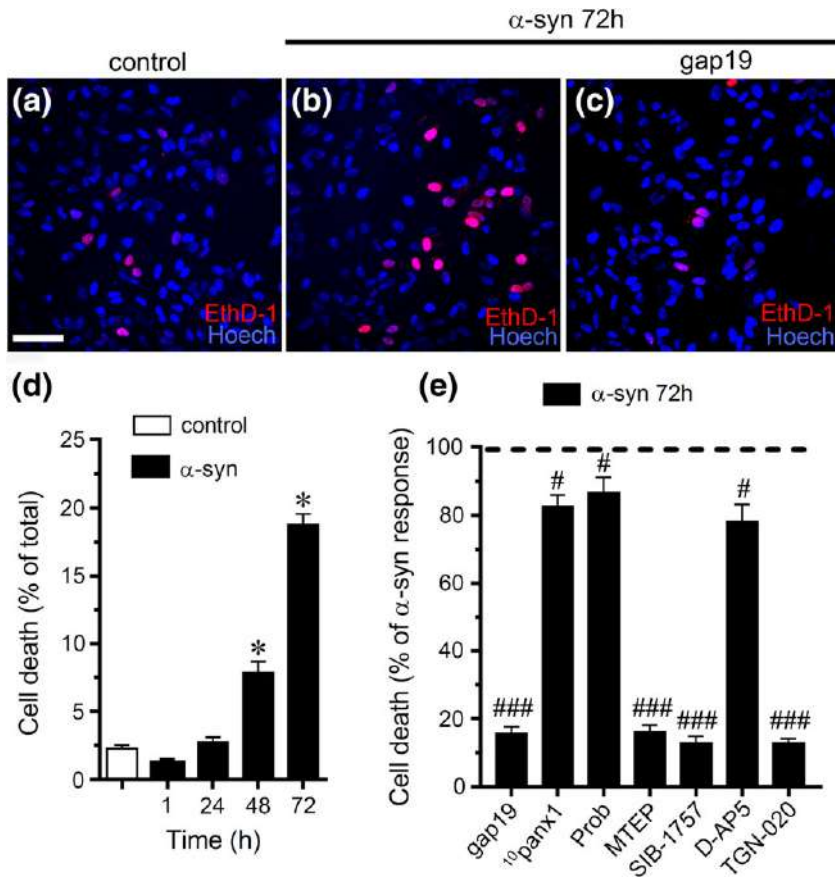


FIGURE 9 Cx43 hemichannel-dependent release of glutamate and further activation of mGluR₅ and AQP4 channels contribute to the α -synuclein-induced astroglial death. (a–c) Representative fluorescence micrographs of Eth-D1 (red) uptake and Hoechst 33342 nuclear staining (blue) by astrocytes under control conditions (a) or treated for 72 hr with 10 nM α -synuclein (b) alone or in combination with 100 μ M gap19 (c). (d) Quantitation of cell death measured by Eth-D1 staining as percentage of total cells identified with Hoechst 33342 by astrocytes under control conditions (white bars) or treated for 1, 24, 48, or 72 hr with 10 nM α -synuclein (black bars). (e) Averaged data normalized to the effect induced by 72 hr of treatment with 10 nM α -synuclein on cell death measured by Eth-D1 staining by astrocytes treated for 72 hr with 10 nM α -synuclein in combination with 100 μ M gap19, 100 μ M 10 panx1, 500 μ M Probenecid, 50 nM MTEP, 5 μ M SIB-1757, 1 μ M D-AP5, and 15 μ M TGN-020. * p < .0001, α -synuclein treatment compared to control conditions, # p < .05, ### p < .0001, effect of pharmacological agents compared to α -synuclein treatment (one-way ANOVA followed by Tukey's post hoc test). Data were obtained from at least three independent experiments with three or more repeats each one. Calibration bar = 200 μ m

results indicate that α -synuclein increases the activity of Cx43 hemichannels and Panx1 channels *ex vivo* in brainstem astrocytes by a mechanism involving the stimulation of IL-1 β /TNF- α iNOS/COX₂-dependent pathway(s).

4 | DISCUSSION

In this study, we demonstrated for the first time that α -synuclein activates Cx43 hemichannels and Panx1 channels in astrocytes. This enhanced channel activity occurred by a mechanism involving the activation of IL-1 β /TNF- α and the stimulation of p38 MAPK/iNOS/COX₂/[Ca²⁺]_i-dependent pathways and purinergic/glutamatergic signaling.

Furthermore, the α -synuclein-induced opening of Cx43 hemichannels and Panx1 channels resulted in profound alterations in [Ca²⁺]_i dynamics, NO production, gliotransmitter release, mitochondrial morphology, and astrocyte survival (Figure 11).

Here, as assayed by Etd uptake, we showed that α -synuclein increases in a time and concentration-dependent manner, the activity of Cx43 hemichannels and Panx1 channels in primary cortical astrocytes. Indeed, the α -synuclein-induced Etd uptake in astrocytes was drastically blocked by Tat-L2, gap19, probenecid, and 10 panx1 or by down-regulation of Cx43 or Panx1, indicating that both Cx43 hemichannels and Panx1 channels were the principal responsible for this response. These findings are in agreement with the increased activity described for both channels in astrocytes exposed to pathological scenarios

FIGURE 8 α -Synuclein alters ATP-dependent Ca²⁺ dynamics in astrocytes by a mechanism implicating the opening of Cx43 hemichannels and Panx1 channels. (a–d) Representative photomicrographs of basal (a, c) or 500 μ M ATP-induced (b, d) Ca²⁺ signal denoted as Fura-2 ratio (340/380 nm excitation) of astrocytes under control conditions (a, b) or treated for 48 hr with 10 nM α -synuclein (c, d). Calibration bar: 100 μ m. (e–i) Representative plots of relative changes in Ca²⁺ signal over time induced by 500 μ M ATP (green horizontal line) in astrocytes under control conditions (e) or treated for 48 hr with 10 nM α -synuclein (f) alone or in combination with the following agents: 100 μ M Tat-L2 (g), 100 μ M gap19 (h), and 100 μ M 10 panx1 (i). (j–n) averaged data of basal Fura-2AM ratio (j), ATP-induced peak amplitude normalized to basal Fura-2AM ratio (k), integrated ATP-induced Fura-2AM ratio response (l), and altered basal Fura-2AM ratio (m) by astrocytes under control conditions (white bars) or treated for different periods (1, 24, 48, and 72 hr) with 10 nM α -synuclein (black bars). (n–p) Averaged data of ATP-induced peak amplitude normalized to basal Fura-2AM ratio (n), integrated ATP-induced Fura-2AM ratio response (o) and altered basal Fura-2AM ratio (p) by astrocytes under control conditions (white bars) or treated for different periods (1, 24, 48, and 72 hr) with 10 nM α -synuclein (black bars) alone or in combination with the following agents: 100 μ M Tat-L2, 100 μ M gap19 and 100 μ M 10 panx1. * p < .05, ** p < .01, α -synuclein treatment compared to control conditions, # p < .01, effect of pharmacological agents compared to α -synuclein treatment (one-way ANOVA followed by Dunnett's post hoc test). Data were obtained from at least three independent experiments with three or more repeats each one (\geq 35 cells analyzed for each repeat) [Color figure can be viewed at wileyonlinelibrary.com]

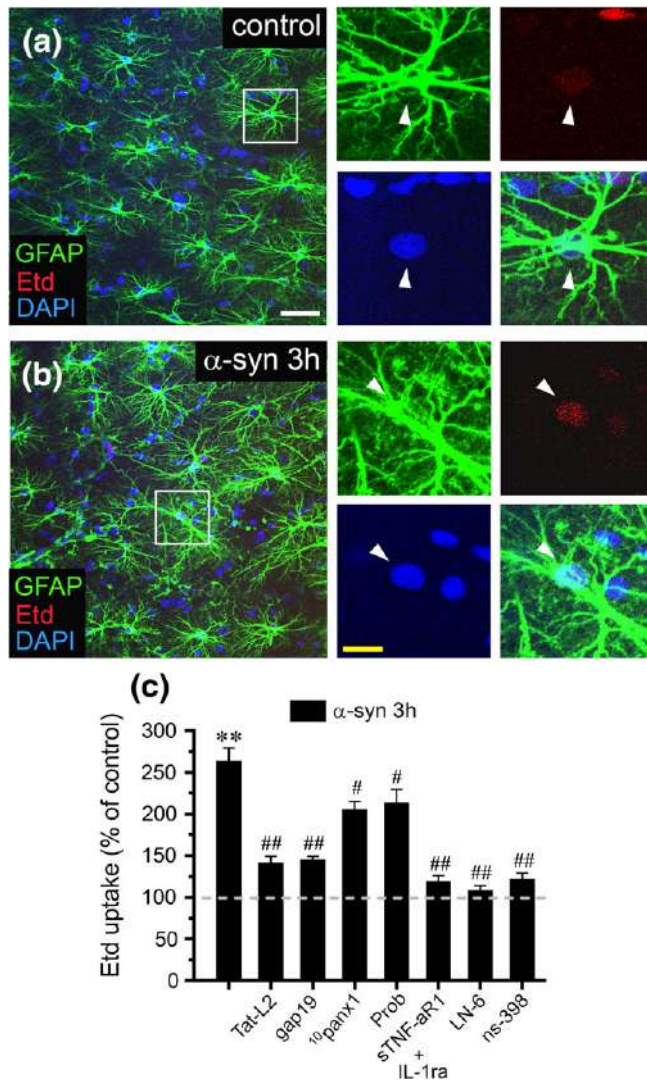


FIGURE 10 α -Synuclein increases the activity of Cx43 hemichannels and Panx1 channels in brainstem astrocytes ex vivo. (a,b) Representative images of DAPI staining (blue) and Etd uptake (red) in GFAP-positive astrocytes (green) from the intermediate reticular formation of acute brainstem slices under control conditions (a) or after 3 hr of treatment with 10 nM α -synuclein (b). Insets of astrocytes were taken from the area depicted within the white squares in a and b. (c) Averaged Etd uptake ratio normalized with control condition (dashed line) by astrocytes from acute brainstem slices after 3 hr of treatment with 10 nM α -synuclein alone or in combination with the following blockers: 100 μ M Tat-L2, 100 μ M gap19, 100 μ M ¹⁰panx1, 500 μ M Probenecid (Prob), 100 ng/mL of IL-1ra + 100 ng/mL of sTNF- α R1, 1 μ M L-N6 or 5 μ M ns-398. ** $p < .001$, α -synuclein compared to control; # $p < .001$, ## $p < .005$; effect of pharmacological agents compared to α -synuclein treatment (one-way ANOVA followed by Dunnett's post hoc test). Data were obtained from at least three independent experiments (≥ 42 cells analyzed for each independent experiment). Calibration bars: White bar = 180 μ m and yellow bar: 45 μ m [Color figure can be viewed at wileyonlinelibrary.com]

including prenatal nicotine and postnatal high-fat diet (Orellana et al., 2014), restraint stress (Orellana et al., 2015), epileptic seizures (Santiago et al., 2011), prenatal LPS exposure (Avendano et al., 2015), spinal cord

injury (Garre, Yang, Bukauskas, & Bennett, 2016), and acute infection (Karpuk et al., 2011).

How does α -synuclein treatment cause the opening of Cx43 hemichannels and Panx1 channels in astrocytes? A growing body of evidence suggests that α -synuclein signaling triggers a long-lasting activation of astrocytes and thereof a wide-range production of inflammatory mediators, including IL-1 β and TNF- α (Chavarria, Rodriguez-Bottero, Quijano, Cassina, & Souza, 2018; Fellner et al., 2013). In fact, the expression of both cytokines is increased in postmortem tissue of patients suffering α -synucleinopathies (Garcia-Esparcia, Llorens, Carmona, & Ferrer, 2014; Nagatsu, Mogi, Ichinose, & Togari, 2000) and their production has been implicated in the opening of astroglial hemichannels and pannexons (Avendano et al., 2015; Retamal et al., 2007). In agreement with these antecedents, we observed that α -synuclein augments astroglial production of IL-1 β and TNF- α , whereas inhibition of IL-1 β /TNF- α signaling prominently tackled the α -synuclein-induced Cx43 hemichannel and Panx1 channel activity. In the same line, astrocytes treated with the concentrations of IL-1 β and TNF- α measured upon treatment with α -synuclein displayed an Etd uptake comparable to that triggered by α -synuclein.

IL-1 β and TNF- α enhance the activity of astrocyte Cx43 hemichannels by stimulating a p38 MAPK-mediated pathway and eliciting the NO-dependent S-nitrosylation of Cx43 (Avendano et al., 2015; Retamal et al., 2006, 2007). Here, we found that α -synuclein increases the production of NO by astrocytes, while blockade of both p38 MAPK and iNOS greatly reduced the α -synuclein-induced-Etd uptake. On the other hand, it is known that COXs and PGE₂ receptor EP₁ activation, as well as [Ca²⁺]_i, are required for the opening of Cx43 hemichannels and Panx1 channels triggered during inflammatory conditions (Avendano et al., 2015; Orellana et al., 2014; Orellana, Montero, & Von Bernhardi, 2013; Saez et al., 2018). In this line, we noticed that BAPTA or selective blockade of COX₂ but not COX₁ or PGE₂ receptor EP₁, dramatically abrogated the α -synuclein-induced hemichannel/pannexon opening. Taken together all above results harmonize with the fact that α -synuclein induces the production of IL-1 β and TNF- α , as well as the activation of p38MAPK, iNOS, and COX₂ in astrocytes (Rannikko, Weber, & Kahle, 2015; Yu et al., 2018; Figure 11). A parallel mechanism of hemichannel and pannexon modulation to that resulting from covalent modifications (e.g., phosphorylation and/or S-nitrosylation) or changes in [Ca²⁺]_i is the sorting of channels to the cell surface. Here, we observed that α -synuclein did not alter surface levels of Cx43 and Panx1, suggesting that other mechanisms rather than changes in surface expression of these proteins are likely involved in the regulation of Cx43 hemichannel and Panx1 channels activity elicited by α -synuclein.

Astrocyte hemichannels and gap junction channels are oppositely activated during inflammatory scenarios (De Bock et al., 2014). Consistent with this, we observed that the opening of astrocyte Cx43 hemichannels caused by α -synuclein was accompanied by a reduction in astrocyte coupling, as detected by intercellular LY diffusion. Astrocyte gap junction coupling underpins the spreading of intracellular K⁺, Na⁺, and Ca²⁺ (Langer, Stephan, Theis, & Rose, 2012; Scemes, Dermietzel, & Spray, 1998; Wallraff et al., 2006), thus participating in

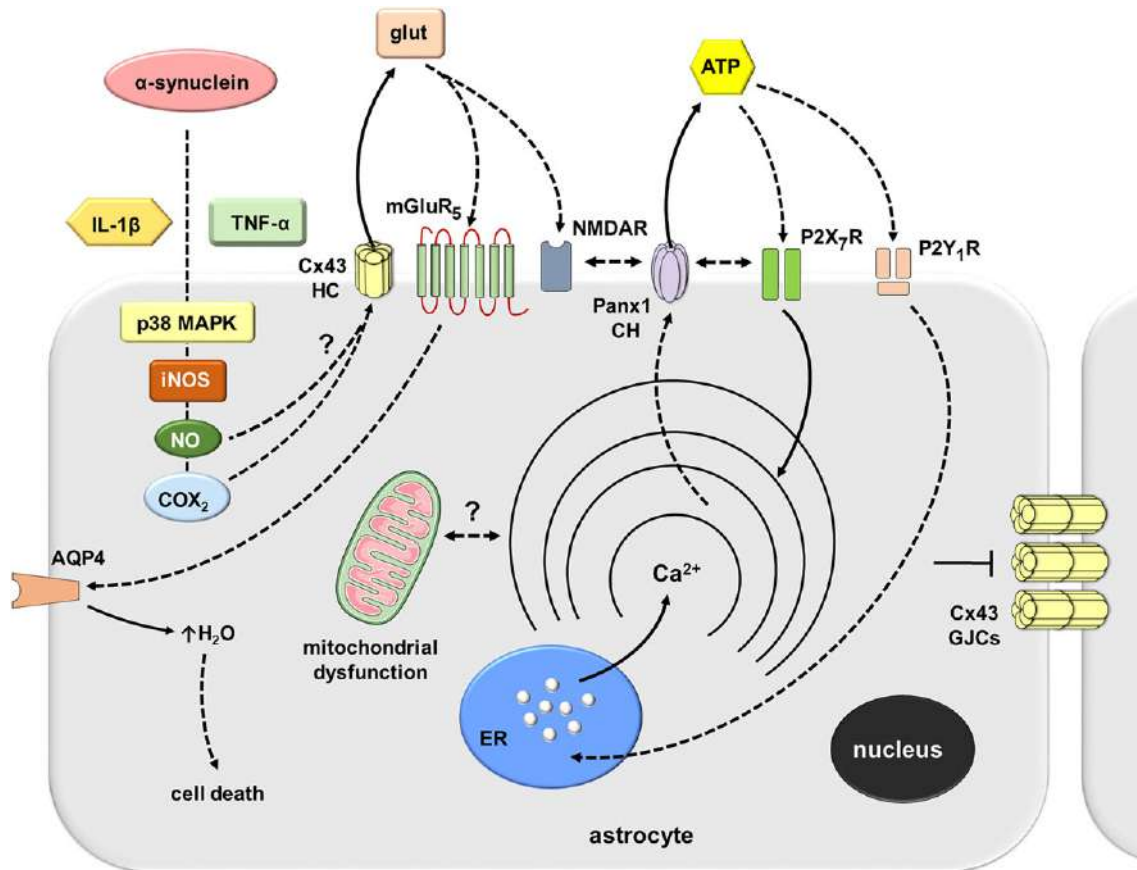


FIGURE 11 Schematic diagram showing the possible pathways involved in the α -synuclein-induced activation of Cx43 hemichannels/Panx1 channels and its consequences for astroglial function. Upon stimulation with α -synuclein, astrocytes respond with intracellular signal transduction that possibly involve the release of IL-1 β /TNF- α associated with the p38 MAPK and iNOS activation, NO production, and further stimulation of COX₂. The latter likely induces unknown mechanisms that cause opening of Cx43 hemichannels enabling the release of glutamate. Glutamate released via Cx43 hemichannels activates NMDA receptors resulting in the opening of Panx1 channels possibly through phosphorylation of Panx1 by Src family kinases. Opening of Panx1 channels allow the release of ATP that stimulates P2X₇ receptors, and its degradation to ADP may activate P2Y₁ receptors. These events trigger the influx of extracellular Ca²⁺ and activation of IP₃ receptors and further release of Ca²⁺ stored in the endoplasmic reticulum. The later could trigger an unknown self-perpetuating mechanism, in which [Ca²⁺]_i could reactivate Panx1 channels and likely Cx43 hemichannels (not depicted). Relevantly, modulation of [Ca²⁺]_i dynamics evoked by Cx43 hemichannel/Panx1 channel signaling may alter mitochondrial morphology and NO production (not depicted). Furthermore, Cx43 hemichannel-dependent release of glutamate triggers the activation of mGluR₅, which for an unknown mechanism could result in the opening of AQP4 and subsequent osmotic unbalance and cell death. In parallel, α -synuclein also reduces astrocyte-astrocyte gap junctional communication [Color figure can be viewed at wileyonlinelibrary.com]

K⁺ buffering, maintenance of neuronal membrane potential and coordination of large populations of astrocytes, all processes being critical for synaptic transmission (Chever, Dossi, Pannasch, Derangeon, & Rouach, 2016; Pannasch et al., 2011, 2014). Additionally, Cx43 gap junctions mediate glucose and lactate trafficking among astrocytes (Ball, Gandhi, Thrash, Cruz, & Dienel, 2007; Rouach, Koulakoff, Abudara, Willecke, & Giaume, 2008), whose actively provide glucose to neurons when they needed and remove lactate from high activity areas (Gandhi, Cruz, Ball, & Dienel, 2009). With this in mind, a reduction in astroglial gap junctional coupling may constitute a crucial step in the pathogenesis and progression of α -synucleinopathies.

Here, we found that uncoupling between astrocytes did not depend on modifications in Cx43 levels or phosphorylation state detectable by changes in electrophoretic mobility, because Cx43 total levels and pattern of immunoreactive bands were equivalent in α -synuclein-stimulated

and control astrocytes. Given that changes in the phosphorylation of Cx43 not necessarily correlate with a shift in its electrophoretic mobility (Solan & Lampe, 2009), we also analyzed the phosphorylation of Cx43 at S368, a residue crucial for the PKC-mediated reduction in gap junction channel conductance and selectivity (Ek-Vitorin et al., 2006; Lampe et al., 2000). Densitometric analysis revealed that α -synuclein did not alter the phosphorylation of Cx43 at S368 compared to control conditions, revealing that α -synuclein-induced uncoupling takes place by a different mechanism. Nevertheless, at the moment, we cannot rule out whether other specific Cx43 phosphorylations could be involved. On the other hand, confocal immunofluorescence labeling revealed no apparent differences in the distribution of structures compatible with gap junction plaques in astrocytes stimulated with α -synuclein, implicating that internalization or degradation of gap junctions do not account for the astrocyte uncoupling.

Glutamate and ATP play crucial roles on astrocyte-to-neuron signaling, but at high synaptic concentrations, they can cause excitotoxicity (Arbeloa, Perez-Samartin, Gottlieb, & Matute, 2012; Ashpole et al., 2013; Lau & Tymianski, 2010). Here, we found that α -synuclein elevates the extracellular levels of glutamate and ATP by a mechanism implicating the activation of Cx43 hemichannels, NMDA receptors, Panx1 channels, and P2X₇/P2Y₁ receptors in astrocytes (Figure 11). Particularly, the inhibition of NMDA and P2X₇/P2Y₁ receptors totally suppressed the α -synuclein-evoked release of ATP but not glutamate. The latter suggests that release of glutamate occurred upstream to the release of ATP evoked by glutamatergic and purinergic signaling. Importantly, probenecid did not cause an additive reduction in the α -synuclein-induced Etd uptake when astrocytes were treated with inhibitors of NMDA and P2X₇/P2Y₁ receptors, indicating that Panx1 channel opening could operate via glutamatergic and purinergic signaling. This leads us to speculate that the release of glutamate likely causes the Panx1 channel-dependent release of ATP via activation of NMDA receptors (Figure 11). The latter may be potentiated by the positive feedback loop linked to ATP-dependent stimulation of P2X₇/P2Y₁ receptors (Figure 11). Supporting this line of thought, the release ATP takes place by the activation of Panx1 channels (Iglesias et al., 2009) and their opening depends on NMDA and P2X₇/P2Y₁ receptor signaling (Iglesias et al., 2009; Locovei et al., 2006; Weilingner et al., 2012). Of note, the α -synuclein-evoked Etd uptake and release of glutamate and ATP were completely abrogated by inhibition or downregulation of Cx43 hemichannels. This possibly reflects that the Cx43 hemichannel-dependent release of glutamate causes the release of ATP via Panx1 channels following the stimulation of NMDA receptors (Figure 11).

ATP produces a biphasic $[Ca^{2+}]_i$ mobilization in astrocytes: The release of internal Ca^{2+} (first spike) and Ca^{2+} influx from the extracellular compartment (sustained response; Neary et al., 1991). The first spike in ATP-evoked $[Ca^{2+}]_i$ mobilization relies on P2Y receptors, whereas the second sustained response occurs due to P2X receptors. Here, we observed that after ATP stimulation, control astrocytes showed a prominent Ca^{2+} signal peak that was followed by a sustained response. On the contrary, α -synuclein-stimulated astrocytes exhibited reduced ATP-evoked $[Ca^{2+}]_i$ mobilizations compared to those untreated, specifically, concerning to peak amplitude, integrated area, and sustained signal. Of note, in terms of basal levels of $[Ca^{2+}]_i$, α -synuclein-treated astrocytes were not significantly different of their control counterparts, suggesting that α -synuclein is affecting mainly ATP-mediated Ca^{2+} dynamics that could depend on the inflammatory profile of astrocytes. It is known that Ca^{2+} dynamics modulate mitochondrial dynamics in astrocytes (Jackson & Robinson, 2015), whereas α -synuclein disturbs the function and morphology of mitochondria (Gustafsson et al., 2017; Lindstrom et al., 2017). In agreement with the latter, we noticed that α -synuclein greatly reduced the size of mitochondria by a mechanism involving the activation of both Cx43 hemichannels and Panx1 channels in astrocytes.

In this study, we observed that astrocytes treated with α -synuclein exhibited a significant decrease in cell survival, the latter response was strongly prevented by the blockade of Cx43 hemichannels rather than Panx1 channels. Relevantly, a recent study demonstrated that AQP4

water channel is crucial for the glutamate-induced astrocyte swelling caused by mGluR₅ activation (Shi et al., 2017). Consistent with this, we observed that α -synuclein-evoked astrocyte death was strongly prevented by the blockade of both AQP4 or mGluR₅, whereas inhibition of NMDA receptors resulted in similar weak protection than Panx1 channel blockers. We speculate that Cx43 hemichannel-dependent release of glutamate and further activation of mGluR₅ and opening of AQP4 water channels is a crucial step in the astrocyte death induced by α -synuclein (Figure 11). NMDA receptor signaling linked to the opening of Panx1 channels could also contribute to astrocyte death as has been demonstrated previously in neurons (Weilingner et al., 2012).

Here we observed that inhibition of Cx43 hemichannels or Panx1 channels counteracted the α -synuclein-evoked alterations in NO production, ATP-mediated $[Ca^{2+}]_i$ dynamics, and mitochondrial morphology. Of note, despite that hemichannel/pannexon activity has been linked to astroglial cytokine production (Wei et al., 2016), the α -synuclein-induced release of IL-1 β and TNF- α did not depend on the opening of Cx43 hemichannels and Panx1 channels, as Tat-L2, gap19 or ¹⁰panx1 failed in to prevent this response. In addition, we show that α -synuclein increased the activity of astrocyte Cx43 hemichannels and Panx1 channels in acute slices of the brainstem, a region where α -synucleinopathies predominate (Seidel et al., 2015). The combination of this integrated preparation, where all cell types are present, allowed us to confirm the effect of α -synuclein on hemichannel/pannexon activity found in astrocyte cultures. Altogether, these findings argue for an α -synuclein-induced inflammatory mechanism with hemichannel/pannexon activation taking place in the early phases of astroglial dysfunction, and being consequences of this process: (a) the augment of NO production, (b) the alterations of ATP-mediated $[Ca^{2+}]_i$ dynamics, (c) the reduction in mitochondrial size, and (d) the decrease of astrocyte survival (Figure 11).

In conclusion, our study reveals a new mechanism by which α -synuclein impairs astrocyte function involving the sequential stimulation of inflammatory pathways that further increase the opening of astroglial hemichannels and pannexons. The latter mechanism could provide a solid basis for determining alternative pharmacological strategies aiming at preserving astrocyte function and neuronal survival during the progression of different α -synucleinopathies.

ACKNOWLEDGMENTS

This work was supported by the Fondo Nacional de Desarrollo Científico y Tecnológico (FONDECYT) Grant 1160710 (to JAO), 1170441 (to RAQ), the Comisión Nacional de Investigación Científica y Tecnológica (CONICYT) and Programa de Investigación Asociativa (PIA) Grant Anillo de Ciencia y Tecnología ACT1411 (to JAO). The authors declare no conflict of interest.

ORCID

Juan A. Orellana  <https://orcid.org/0000-0003-4076-207X>

REFERENCES

- Abudara, V., Bechberger, J., Freitas-Andrade, M., De Bock, M., Wang, N., Bultynck, G., ... Giaume, C. (2014). The connexin43 mimetic peptide Gap19 inhibits hemichannels without altering gap junctional communication in astrocytes. *Frontiers in Cellular Neuroscience*, 8, 306.
- Abudara, V., Roux, L., Dallerac, G., Matias, I., Dulong, J., Mothet, J. P., ... Giaume, C. (2015). Activated microglia impairs neuroglial interaction by opening Cx43 hemichannels in hippocampal astrocytes. *Glia*, 63, 795–811.
- Agulhon, C., Sun, M. Y., Murphy, T., Myers, T., Lauderdale, K., & Fiocco, T. A. (2012). Calcium signaling and Gliotransmission in Normal vs. reactive astrocytes. *Frontiers in Pharmacology*, 3, 139.
- Arbeloa, J., Perez-Samartin, A., Gottlieb, M., & Matute, C. (2012). P2X7 receptor blockade prevents ATP excitotoxicity in neurons and reduces brain damage after ischemia. *Neurobiology of Disease*, 45, 954–961.
- Ashpole, N. M., Chawla, A. R., Martin, M. P., Brustovetsky, T., Brustovetsky, N., & Hudmon, A. (2013). Loss of calcium/calmodulin-dependent protein kinase II activity in cortical astrocytes decreases glutamate uptake and induces neurotoxic release of ATP. *The Journal of Biological Chemistry*, 288, 14599–14611.
- Avendano, B. C., Montero, T. D., Chavez, C. E., Von Bernhardi, R., & Orellana, J. A. (2015). Prenatal exposure to inflammatory conditions increases Cx43 and Panx1 unopposed channel opening and activation of astrocytes in the offspring effect on neuronal survival. *Glia*, 63, 2058–2072.
- Ball, K. K., Gandhi, G. K., Thrash, J., Cruz, N. F., & Dienel, G. A. (2007). Astrocytic connexin distributions and rapid, extensive dye transfer via gap junctions in the inferior colliculus: Implications for [(14)C]glucose metabolite trafficking. *Journal of Neuroscience Research*, 85, 3267–3283.
- Baroja-Mazo, A., Barbera-Cremades, M., & Pelegrin, P. (2013). The participation of plasma membrane hemichannels to purinergic signaling. *Biochimica et Biophysica Acta*, 1828, 79–93.
- Bendor, J. T., Logan, T. P., & Edwards, R. H. (2013). The function of alpha-synuclein. *Neuron*, 79, 1044–1066.
- Chavarria, C., Rodriguez-Bottero, S., Quijano, C., Cassina, P., & Souza, J. M. (2018). Impact of monomeric, oligomeric and fibrillar alpha-synuclein on astrocyte reactivity and toxicity to neurons. *The Biochemical Journal*, 475, 3153–3169.
- Chever, O., Dossi, E., Pannasch, U., Derangeon, M., & Rouach, N. (2016). Astroglial networks promote neuronal coordination. *Science Signaling*, 9, ra6.
- Chever, O., Lee, C. Y., & Rouach, N. (2014). Astroglial connexin43 hemichannels tune basal excitatory synaptic transmission. *The Journal of Neuroscience*, 34, 11228–11232.
- Chi, Y., Gao, K., Li, K., Nakajima, S., Kira, S., Takeda, M., & Yao, J. (2014). Purinergic control of AMPK activation by ATP released through connexin 43 hemichannels—Pivotal roles in hemichannel-mediated cell injury. *Journal of Cell Science*, 127, 1487–1499.
- Crow, D. S., Beyer, E. C., Paul, D. L., Kobe, S. S., & Lau, A. F. (1990). Phosphorylation of connexin43 gap junction protein in uninfected and Rous sarcoma virus-transformed mammalian fibroblasts. *Molecular and Cellular Biology*, 10, 1754–1763.
- De Bock, M., Decrock, E., Wang, N., Bol, M., Vinken, M., Bultynck, G., & Leybaert, L. (2014). The dual face of connexin-based astroglial Ca²⁺ communication: A key player in brain physiology and a prime target in pathology. *Biochimica et Biophysica Acta*, 1843, 2211–2232.
- De Bock, M., Wang, N., Bol, M., Decrock, E., Ponsaerts, R., Bultynck, G., ... Leybaert, L. (2012). Connexin 43 hemichannels contribute to cytoplasmic Ca²⁺ oscillations by providing a bimodal Ca²⁺-dependent Ca²⁺ entry pathway. *The Journal of Biological Chemistry*, 287, 12250–12266.
- Diogenes, M. J., Dias, R. B., Rombo, D. M., Vicente Miranda, H., Maiolino, F., Guerreiro, P., ... Outeiro, T. F. (2012). Extracellular alpha-synuclein oligomers modulate synaptic transmission and impair LTP via NMDA-receptor activation. *The Journal of Neuroscience*, 32, 11750–11762.
- Ek-Vitorin, J. F., King, T. J., Heyman, N. S., Lampe, P. D., & Burt, J. M. (2006). Selectivity of connexin 43 channels is regulated through protein kinase C-dependent phosphorylation. *Circulation Research*, 98, 1498–1505.
- Fellner, L., Irschick, R., Schanda, K., Reindl, M., Klimaschewski, L., Poewe, W., ... Stefanova, N. (2013). Toll-like receptor 4 is required for alpha-synuclein dependent activation of microglia and astroglia. *Glia*, 61, 349–360.
- Fiori, M. C., Figueroa, V., Zoghbi, M. E., Saez, J. C., Reuss, L., & Altenberg, G. A. (2012). Permeation of calcium through purified connexin 26 hemichannels. *The Journal of Biological Chemistry*, 287, 40826–40834.
- Gajardo-Gomez, R., Labra, V. C., Maturana, C. J., Shoji, K. F., Santibanez, C. A., Saez, J. C., ... Orellana, J. A. (2017). Cannabinoids prevent the amyloid beta-induced activation of astroglial hemichannels: A neuroprotective mechanism. *Glia*, 65, 122–137.
- Gandhi, G. K., Cruz, N. F., Ball, K. K., & Dienel, G. A. (2009). Astrocytes are poised for lactate trafficking and release from activated brain and for supply of glucose to neurons. *Journal of Neurochemistry*, 111, 522–536.
- Garcia-Esparcia, P., Llorens, F., Carmona, M., & Ferrer, I. (2014). Complex deregulation and expression of cytokines and mediators of the immune response in Parkinson's disease brain is region dependent. *Brain Pathology*, 24, 584–598.
- Garre, J. M., Yang, G., Bukauskas, F. F., & Bennett, M. V. (2016). FGF-1 triggers Pannexin-1 Hemichannel opening in spinal astrocytes of rodents and promotes inflammatory responses in acute spinal cord slices. *The Journal of Neuroscience*, 36, 4785–4801.
- Gustafsson, G., Lindstrom, V., Rostami, J., Nordstrom, E., Lannfelt, L., Bergstrom, J., ... Erlandsson, A. (2017). Alpha-synuclein oligomer-selective antibodies reduce intracellular accumulation and mitochondrial impairment in alpha-synuclein exposed astrocytes. *Journal of Neuroinflammation*, 14, 241.
- Iglesias, R., Dahl, G., Qiu, F., Spray, D. C., & Scemes, E. (2009). Pannexin 1: The molecular substrate of astrocyte "hemichannels". *The Journal of Neuroscience*, 29, 7092–7097.
- Ishikawa, M., Iwamoto, T., Nakamura, T., Doyle, A., Fukumoto, S., & Yamada, Y. (2011). Pannexin 3 functions as an ER Ca²⁺ channel, hemichannel, and gap junction to promote osteoblast differentiation. *The Journal of Cell Biology*, 193, 1257–1274.
- Jackson, J. G., & Robinson, M. B. (2015). Reciprocal regulation of mitochondrial dynamics and calcium signaling in astrocyte processes. *The Journal of Neuroscience*, 35, 15199–15213.
- Johnson, R. G., Le, H. C., Evenson, K., Loberg, S. W., Myslajek, T. M., Prabhu, A., ... Sheridan, J. D. (2016). Connexin Hemichannels: Methods for dye uptake and leakage. *The Journal of Membrane Biology*, 249, 713–741.
- Karpuk, N., Burkovetskaya, M., Fritz, T., Angle, A., & Kielian, T. (2011). Neuroinflammation leads to region-dependent alterations in astrocyte gap junction communication and hemichannel activity. *The Journal of Neuroscience*, 31, 414–425.
- Klegeris, A., Giasson, B. I., Zhang, H., Maguire, J., Pelech, S., & McGeer, P. L. (2006). Alpha-synuclein and its disease-causing mutants induce ICAM-1 and IL-6 in human astrocytes and astrocytoma cells. *The FASEB Journal*, 20, 2000–2008.
- Koob, A. O., Paulino, A. D., & Masliah, E. (2010). GFAP reactivity, apolipoprotein E redistribution and cholesterol reduction in human astrocytes treated with alpha-synuclein. *Neuroscience Letters*, 469, 11–14.
- Lampe, P. D., & Lau, A. F. (2004). The effects of connexin phosphorylation on gap junctional communication. *The International Journal of Biochemistry & Cell Biology*, 36, 1171–1186.
- Lampe, P. D., Tenbroek, E. M., Burt, J. M., Kurata, W. E., Johnson, R. G., & Lau, A. F. (2000). Phosphorylation of connexin43 on serine368 by protein kinase C regulates gap junctional communication. *The Journal of Cell Biology*, 149, 1503–1512.
- Langer, J., Stephan, J., Theis, M., & Rose, C. R. (2012). Gap junctions mediate intercellular spread of sodium between hippocampal astrocytes in situ. *Glia*, 60, 239–252.

- Lau, A., & Tymianski, M. (2010). Glutamate receptors, neurotoxicity and neurodegeneration. *Pflügers Archiv*, *460*, 525–542.
- Leybaert, L., Lampe, P. D., Dhein, S., Kwak, B. R., Ferdinandy, P., Beyer, E. C., ... Schulz, R. (2017). Connexins in cardiovascular and neurovascular health and disease: Pharmacological implications. *Pharmacological Reviews*, *69*, 396–478.
- Lindstrom, V., Gustafsson, G., Sanders, L. H., Howlett, E. H., Sigvardson, J., Kasrayan, A., ... Erlandsson, A. (2017). Extensive uptake of alpha-synuclein oligomers in astrocytes results in sustained intracellular deposits and mitochondrial damage. *Molecular and Cellular Neurosciences*, *82*, 143–156.
- Liu, M., Qin, L., Wang, L., Tan, J., Zhang, H., Tang, J., ... Wang, C. (2018). Alphasynuclein induces apoptosis of astrocytes by causing dysfunction of the endoplasmic reticulumGolgi compartment. *Molecular Medicine Reports*, *18*, 322–332.
- Locovei, S., Wang, J., & Dahl, G. (2006). Activation of pannexin 1 channels by ATP through P2Y receptors and by cytoplasmic calcium. *FEBS Letters*, *580*, 239–244.
- Meunier, C., Wang, N., Yi, C., Dallerac, G., Ezan, P., Koulakoff, A., ... Giaume, C. (2017). Contribution of Astroglial Cx43 Hemichannels to the modulation of glutamatergic currents by D-serine in the mouse prefrontal cortex. *The Journal of Neuroscience*, *37*, 9064–9075.
- Montero, T. D., & Orellana, J. A. (2015). Hemichannels: New pathways for gliotransmitter release. *Neuroscience*, *286*, 45–59.
- Motori, E., Puyal, J., Toni, N., Ghanem, A., Angeloni, C., Malaguti, M., ... Bergami, M. (2013). Inflammation-induced alteration of astrocyte mitochondrial dynamics requires autophagy for mitochondrial network maintenance. *Cell Metabolism*, *18*, 844–859.
- Mugisho, O. O., Green, C. R., Kho, D. T., Zhang, J., Graham, E. S., Acosta, M. L., & Rupenthal, I. D. (2018). The inflammasome pathway is amplified and perpetuated in an autocrine manner through connexin43 hemichannel mediated ATP release. *Biochimica et Biophysica Acta - General Subjects*, *1862*, 385–393.
- Nagatsu, T., Mogi, M., Ichinose, H., & Togari, A. (2000). Changes in cytokines and neurotrophins in Parkinson's disease. *Journal of Neural Transmission. Supplementum*, *60*, 277–290.
- Neary, J. T., Laskey, R., Van Breemen, C., Blicharska, J., Norenberg, L. O., & Norenberg, M. D. (1991). ATP-evoked calcium signal stimulates protein phosphorylation/dephosphorylation in astrocytes. *Brain Research*, *566*, 89–94.
- Nielsen, B. S., Hansen, D. B., Ransom, B. R., Nielsen, M. S., & Macaulay, N. (2017). Connexin Hemichannels in astrocytes: An assessment of controversies regarding their functional characteristics. *Neurochemical Research*, *42*, 2537–2550.
- Orellana, J. A., Busso, D., Ramirez, G., Campos, M., Rigotti, A., Eugenin, J., & Von Bernhardi, R. (2014). Prenatal nicotine exposure enhances Cx43 and Panx1 unopposed channel activity in brain cells of adult offspring mice fed a high-fat/cholesterol diet. *Frontiers in Cellular Neuroscience*, *8*, 403.
- Orellana, J. A., Hernandez, D. E., Ezan, P., Velarde, V., Bennett, M. V., Giaume, C., & Sáez, J. C. (2010). Hypoxia in high glucose followed by reoxygenation in normal glucose reduces the viability of cortical astrocytes through increased permeability of connexin 43 hemichannels. *Glia*, *58*, 329–343.
- Orellana, J. A., Montero, T. D., & Von Bernhardi, R. (2013). Astrocytes inhibit nitric oxide-dependent Ca(2+) dynamics in activated microglia: Involvement of ATP released via pannexin 1 channels. *Glia*, *61*, 2023–2037.
- Orellana, J. A., Moraga-Amaro, R., Diaz-Galarce, R., Rojas, S., Maturana, C. J., Stehberg, J., & Saez, J. C. (2015). Restraint stress increases hemichannel activity in hippocampal glial cells and neurons. *Frontiers in Cellular Neuroscience*, *9*, 102.
- Orellana, J. A., Retamal, M. A., Moraga-Amaro, R., & Stehberg, J. (2016). Role of Astroglial Hemichannels and Pannexons in memory and neurodegenerative diseases. *Frontiers in Integrative Neuroscience*, *10*, 26.
- Orellana, J. A., Shoji, K. F., Abudara, V., Ezan, P., Amigou, E., Sáez, P. J., ... Giaume, C. (2011). Amyloid beta-induced death in neurons involves glial and neuronal hemichannels. *The Journal of Neuroscience*, *31*, 4962–4977.
- Pannasch, U., Freche, D., Dallerac, G., Ghezali, G., Escartin, C., Ezan, P., ... Rouach, N. (2014). Connexin 30 sets synaptic strength by controlling astroglial synapse invasion. *Nature Neuroscience*, *17*, 549–558.
- Pannasch, U., Vargova, L., Reingruber, J., Ezan, P., Holzman, D., Giaume, C., ... Rouach, N. (2011). Astroglial networks scale synaptic activity and plasticity. *Proceedings of the National Academy of Sciences of the United States of America*, *108*, 8467–8472.
- Parzych, K., Zetterqvist, A. V., Wright, W. R., Kirkby, N. S., Mitchell, J. A., & Paul-Clark, M. J. (2017). Differential role of pannexin-1/ATP/P2X7 axis in IL-1beta release by human monocytes. *The FASEB Journal*, *31*, 2439–2445.
- Pekny, M., & Pekna, M. (2014). Astrocyte reactivity and reactive astrogliosis: Costs and benefits. *Physiological Reviews*, *94*, 1077–1098.
- Pelegri, P., & Surprenant, A. (2006). Pannexin-1 mediates large pore formation and interleukin-1beta release by the ATP-gated P2X7 receptor. *The EMBO Journal*, *25*, 5071–5082.
- Perea, G., Navarrete, M., & Araque, A. (2009). Tripartite synapses: Astrocytes process and control synaptic information. *Trends in Neurosciences*, *32*, 421–431.
- Polymeropoulos, M. H., Lavedan, C., Leroy, E., Ide, S. E., Dehejia, A., Dutra, A., ... Nussbaum, R. L. (1997). Mutation in the alpha-synuclein gene identified in families with Parkinson's disease. *Science*, *276*, 2045–2047.
- Ponsaerts, R., De Vuyst, E., Retamal, M., D'hondt, C., Vermeire, D., Wang, N., ... Bultynck, G. (2010). Intramolecular loop/tail interactions are essential for connexin 43-hemichannel activity. *The FASEB Journal*, *24*, 4378–4395.
- Rannikko, E. H., Weber, S. S., & Kahle, P. J. (2015). Exogenous alpha-synuclein induces toll-like receptor 4 dependent inflammatory responses in astrocytes. *BMC Neuroscience*, *16*, 57.
- Retamal, M. A., Cortes, C. J., Reuss, L., Bennett, M. V., & Saez, J. C. (2006). S-nitrosylation and permeation through connexin 43 hemichannels in astrocytes: Induction by oxidant stress and reversal by reducing agents. *Proceedings of the National Academy of Sciences of the United States of America*, *103*, 4475–4480.
- Retamal, M. A., Froger, N., Palacios-Prado, N., Ezan, P., Saez, P. J., Saez, J. C., & Giaume, C. (2007). Cx43 hemichannels and gap junction channels in astrocytes are regulated oppositely by proinflammatory cytokines released from activated microglia. *The Journal of Neuroscience*, *27*, 13781–13792.
- Rouach, N., Koulakoff, A., Abudara, V., Willecke, K., & Giaume, C. (2008). Astroglial metabolic networks sustain hippocampal synaptic transmission. *Science*, *322*, 1551–1555.
- Rovegno, M., Soto, P. A., Saez, P. J., Naus, C. C., Saez, J. C., & Von Bernhardi, R. (2015). Connexin43 hemichannels mediate secondary cellular damage spread from the trauma zone to distal zones in astrocyte monolayers. *Glia*, *63*, 1185–1199.
- Saez, J. C., Contreras-Duarte, S., Gomez, G. I., Labra, V. C., Santibanez, C. A., Gajardo-Gomez, R., ... Orellana, J. A. (2018). Connexin 43 Hemichannel activity promoted by pro-inflammatory cytokines and high glucose alters endothelial cell function. *Frontiers in Immunology*, *9*, 1899.
- Saez, P. J., Orellana, J. A., Vega-Riveros, N., Figueroa, V. A., Hernandez, D. E., Castro, J. F., ... Saez, J. C. (2013). Disruption in connexin-based communication is associated with intracellular Ca(2+)-signal alterations in astrocytes from Niemann-Pick type C mice. *PLoS One*, *8*, e71361.
- Salameh, A., Blanke, K., & Dhein, S. (2013). Mind the gap! Connexins and pannexins in physiology, pharmacology and disease. *Frontiers in Pharmacology*, *4*, 144.
- Santiago, M. F., Veliskova, J., Patel, N. K., Lutz, S. E., Caille, D., Charollais, A., ... Scemes, E. (2011). Targeting pannexin1 improves seizure outcome. *PLoS One*, *6*, e25178.

- Scemes, E., Dermietzel, R., & Spray, D. C. (1998). Calcium waves between astrocytes from Cx43 knockout mice. *Glia*, 24, 65–73.
- Schalper, K. A., Palacios-Prado, N., Retamal, M. A., Shoji, K. F., Martinez, A. D., & Saez, J. C. (2008). Connexin hemichannel composition determines the FGF-1-induced membrane permeability and free $[Ca^{2+}]_i$ responses. *Molecular Biology of the Cell*, 19, 3501–3513.
- Seidel, K., Mahlke, J., Siswanto, S., Kruger, R., Heinsen, H., Auburger, G., ... Rub, U. (2015). The brainstem pathologies of Parkinson's disease and dementia with Lewy bodies. *Brain Pathology*, 25, 121–135.
- Shi, Z., Zhang, W., Lu, Y., Xu, L., Fang, Q., Wu, M., ... Yuan, F. (2017). Aquaporin 4-mediated glutamate-induced astrocyte swelling is partially mediated through metabotropic glutamate receptor 5 activation. *Frontiers in Cellular Neuroscience*, 11, 116.
- Solan, J. L., & Lampe, P. D. (2009). Connexin43 phosphorylation: Structural changes and biological effects. *The Biochemical Journal*, 419, 261–272.
- Spillantini, M. G., Schmidt, M. L., Lee, V. M., Trojanowski, J. Q., Jakes, R., & Goedert, M. (1997). Alpha-synuclein in Lewy bodies. *Nature*, 388, 839–840.
- Stehberg, J., Moraga-Amaro, R., Salazar, C., Becerra, A., Echeverria, C., Orellana, J. A., ... Retamal, M. A. (2012). Release of gliotransmitters through astroglial connexin 43 hemichannels is necessary for fear memory consolidation in the basolateral amygdala. *The FASEB Journal*, 26, 3649–3657.
- Swierkosz, T. A., Mitchell, J. A., Warner, T. D., Botting, R. M., & Vane, J. R. (1995). Co-induction of nitric oxide synthase and cyclo-oxygenase: Interactions between nitric oxide and prostanoids. *British Journal of Pharmacology*, 114, 1335–1342.
- Takeuchi, H., Jin, S., Wang, J., Zhang, G., Kawanokuchi, J., Kuno, R., ... Suzumura, A. (2006). Tumor necrosis factor- α induces neurotoxicity via glutamate release from hemichannels of activated microglia in an autocrine manner. *The Journal of Biological Chemistry*, 281, 21362–21368.
- Vekrellis, K., Xilouri, M., Emmanouilidou, E., Rideout, H. J., & Stefanis, L. (2011). Pathological roles of alpha-synuclein in neurological disorders. *Lancet Neurology*, 10, 1015–1025.
- Voigt, J., Grosche, A., Vogler, S., Pannicke, T., Hollborn, M., Kohen, L., ... Bringmann, A. (2015). Nonvesicular release of ATP from rat retinal glial (Müller) cells is differentially mediated in response to osmotic stress and glutamate. *Neurochemical Research*, 40, 651–660.
- Volterra, A., Liaudet, N., & Savtchouk, I. (2014). Astrocyte Ca^{2+} signaling: An unexpected complexity. *Nature Reviews. Neuroscience*, 15, 327–335.
- Wallraff, A., Kohling, R., Heinemann, U., Theis, M., Willecke, K., & Steinhauser, C. (2006). The impact of astrocytic gap junctional coupling on potassium buffering in the hippocampus. *The Journal of Neuroscience*, 26, 5438–5447.
- Wang, N., De Bock, M., Decrock, E., Bola, M., Gadicherla, A., Bultynck, G., & Leybaert, L. (2013). Connexin targeting peptides as inhibitors of voltage- and intracellular Ca^{2+} -triggered Cx43 hemichannel opening. *Neuropharmacology*, 75, 506–516.
- Wei, L., Sheng, H., Chen, L., Hao, B., Shi, X., & Chen, Y. (2016). Effect of pannexin-1 on the release of glutamate and cytokines in astrocytes. *Journal of Clinical Neuroscience*, 23, 135–141.
- Weilinger, N. L., Tang, P. L., & Thompson, R. J. (2012). Anoxia-induced NMDA receptor activation opens pannexin channels via Src family kinases. *The Journal of Neuroscience*, 32, 12579–12588.
- Yi, C., Mei, X., Ezan, P., Mato, S., Matias, I., Giaume, C., & Koulakoff, A. (2016). Astroglial connexin43 contributes to neuronal suffering in a mouse model of Alzheimer's disease. *Cell Death and Differentiation*, 23, 1691–1701.
- Yu, W. W., Cao, S. N., Zang, C. X., Wang, L., Yang, H. Y., Bao, X. Q., & Zhang, D. (2018). Heat shock protein 70 suppresses neuroinflammation induced by alpha-synuclein in astrocytes. *Molecular and Cellular Neurosciences*, 86, 58–64.
- Zhang, W., Wang, T., Pei, Z., Miller, D. S., Wu, X., Block, M. L., ... Zhang, J. (2005). Aggregated alpha-synuclein activates microglia: A process leading to disease progression in Parkinson's disease. *The FASEB Journal*, 19, 533–542.

SUPPORTING INFORMATION

Additional supporting information may be found online in the Supporting Information section at the end of this article.

How to cite this article: Díaz EF, Labra VC, Alvear TF, et al. Connexin 43 hemichannels and pannexin-1 channels contribute to the α -synuclein-induced dysfunction and death of astrocytes. *Glia*. 2019;1–22. <https://doi.org/10.1002/glia.23631>